博士論文

論 文 題 目　BAALC potentiates oncogenic ERK pathway through interactions with MEKK1 and KLF4.

（急性骨髄性白血病細胞において BAALC は MEKK1 および KLF4 との相互作用を介して腫瘍形成性 ERK 経路を活性化している）

氏　　名　　　森田　剣

**Contents**


| | |
|---|---|
| Summary | 2 |
| Introduction | 4 |
| Materials and Methods | 9 |
| Results | 23 |
| Discussion | 79 |
| Acknowledgements | 84 |
| References | 86 |
| Tables | 99 |

**Summary**

Although high brain and acute leukemia, cytoplasmic (BAALC) expression is a well-characterized poor prognostic factor in acute myeloid leukemia (AML) patients, neither the exact mechanisms underlying overexpression of BAALC in leukemogenesis and drug resistance nor therapeutic approach against BAALC-high AML have been properly elucidated. Here we report that sustained activation of extracellular signal-regulated kinase (ERK) pathway, induced by the interaction of BAALC and mitogen-activated protein (MAP) kinase kinase kinase 1 (MEKK1), is found to be the hallmark of BAALC-high AML, which leads to accelerated cell cycle progression and development of chemoresistance. We demonstrated that BAALC promotes proliferation of leukemia cells by activating ERK pathway as an adaptor protein, which inhibits the interaction between ERK and mitogen-activated protein (MAP) kinase phosphatase 3 (MKP3/DUSP6). We also elucidated that BAALC induces ERK-mediated chemoresistance through up-regulation of ATP-binding cassette (ABC) transporter genes. Furthermore, BAALC holds Krüppel-like factor 4 (KLF4) in the cytoplasm and inhibits KLF4-dependent differentiation of leukemia cells.

Consequently, MEK inhibition synergizes with KLF4 induction to suppress the growth of AML cells with high BAALC expression both in vitro and in vivo. Our data provide a molecular basis for the role of BAALC in regulating proliferation and differentiation of AML cells and highlight the unique dual function of BAALC as an attractive therapeutic target against BAALC-high AML.

## Introduction

Acute myeloid leukemia (AML) is a clonal disorder characterized by differentiation arrest and accumulation of immature myeloid progenitors in the bone marrow, resulting in hematopoietic failure[1]. In clinical, AML is a highly heterogeneous disease, and responses to therapy can vary widely depending on patient- and disease-related factors. Current therapy for AML consists of chemotherapy and/or hematopoietic stem cell transplant (HSCT) for patients who meet eligibility requirements. Despite the curative potential of HSCT, however, the associated risks preclude many patients from undergoing this procedure. Of patients treated with intensive induction chemotherapy, a considerable proportion do not respond, relapse after initial responses. Disease-related risk factors for these treatment-resistant AML patients have historically been placed undue reliance on karyotype analysis, but recent advances in high-throughput molecular investigation using next-generation sequencers enabled more precise and rational grouping of high-risk AML in view of gene expressions and mutations. In spite of these recent proceedings in the management of AML, more than half of young adult and about 90 % of elderly patients still finally succumb to their disease[2] and few effective treatments exist for these patients outside of HSCT. Thus, novel therapeutic approaches different from conventional chemotherapies, based on deeper understanding in molecular mechanisms of poor-prognostic factors are urgently needed.

To date, several poor prognostic factors for AML have been reported, which include gene mutations in TET2, ASXL1 or DNMT3A[3-5] and overexpression of ERG, EVI1, MN1 or BAALC[6-9]. BAALC was first reported as a novel gene implicated both in neuroectodermal and hematopoietic cell development[10]. In general, overexpression of BAALC is observed in one-forth of AML patients with normal karyotypes[9, 11, 12], and recent reports have shown its adverse impact on the survival of AML patients across all karyotypes[13]. *BAALC*, located on human chromosome 8 at q22.3, encodes at least 8 alternatively spliced transcripts in humans, and *BAALC 1-6-8* is the major isoform expressed in hematopoietic cells[10]. In normal hematopoiesis, the expression of BAALC is limited to the immature fraction, i.e. $CD34^+$ fraction rich in hematopoietic stem and progenitor cells[14]. In a large cohort of patients with AML, high BAALC expression was associated with expressions of stem cell markers[11]. From these facts, it is suggested that BAALC is related to immaturity of hematopoietic cells, but the precise function of BAALC in leukemogenesis is poorly understood.

Aberrant activation of several oncogenic signaling cascades is implicated in AML pathogenesis[15]. Previous reports showed that Ras/Raf/mitogen-activated protein kinase (MEK)/extracellular signal-regulated kinase (ERK) pathway is activated in a significant proportion of AML patients[16] and expected as a potential therapeutic target[17]. However, the antileukemic activity of MEK inhibitor monotherapy in the clinical settings has been modest[18], which necessitates further elucidation of the full picture of the signaling networks, including spatial and temporal relationships of its components and factors that affect their interactions. Among them, Mitogen-activated protein kinase kinase kinase 1 (MEKK1) is necessary for efficient activation of ERK pathway not only as a protein kinase that phosphorylates MEK but as a scaffold protein of key elements in ERK pathway[19]. While previous reports have suggested a fundamental role of MEKK1 in anti-apoptotic function in myeloid cells and successive leukemogenesis[20, 21], little has been reported on how molecular distribution of signaling factors around this essential scaffold protein affects oncogenic signaling cascade in AML.

By contrast, ERK can trigger tumor suppressor pathways as well, such as cellular senescence, apoptosis and differentiation[22-24] in a context-dependent manner. Among them, Krüppel-like factor 4 (KLF4), a member of Krüppel-like family transcription factors, is induced by ERK activation and mediates growth inhibition in human colon cancer cells[25]. Although KLF4 has been shown to enhance stem-cell like properties as one of four iPS factors[26], it has been drawing attention in AML as an essential factor for monocytic differentiation[27]. Furthermore, KLF4 has been reported to possess growth-inhibitory properties in CDX2-driven AML[28]. Based on these findings, anticancer drugs that augment the effect of KLF4 have been newly developed and investigated in clinical and preclinical settings[29-32]. Although promising results from these studies highlight KLF4 as a potential therapeutic target for many malignancies including AML, given the effect of KLF4 is highly context-dependent[33], precise characterization of KLF4 function in each setting is mandatory for proper therapeutic targeting.

In this study, we aimed to investigate the molecular basis of BAALC in leukemia cell proliferation and the therapeutic target for BAALC-high AML. We demonstrate here that through interactions with MEKK1 and KLF4, BAALC potentiates oncogenic ERK pathway while inhibiting ERK-dependent differentiation. This study could also determine whether concurrent MEK inhibition and KLF4 induction would be legitimate therapeutic targets for BAALC-high AML.

## Materials and Methods.

### Mice

NSG mice were purchased from the Jackson Laboratory. Littermates were used as controls in all experiments. All animal experiments were approved by The University of Tokyo Ethics Committee for Animal Experiments and strictly adhered to the guidelines for animal experiments of The University of Tokyo.

### Plasmids and expression constructs

For lentiviral expression of each protein, we cloned cDNA construct of CA-MEK1, MEKK1, MKP3, KLF4, BAALC into CSII-EF-MCS-IRES2-Venus, CSII-EF-MCS-IRES2-hKO1, and CSIV-TRE-Ubc-KT vectors. Deletion mutants of BAALC, KLF4 and MEKK1 were produced by PCR-based mutagenesis from full length BAALC 1-6-8, KLF4 and MEKK1. Each mutant was designed as indicated in the body text, and cloned into MYC-tagged, FLAG-tagged, His-tagged or HA-tagged pcDNA3 expression vectors respectively. All of the PCR products were verified by

DNA sequencing. PCR primers used for the generation of each deletion mutant are listed in Table 1.

**Production and transduction of retrovirus and lentivirus**

To obtain retroviral supernatants, platinum-A (Plat-A) packaging cells were transiently transfected with each retrovirus vector by polyethylenimine (PEI, Sigma-Aldrich), and the viral supernatants were collected 48 hours after transfection and used immediately for infection. Virus was transduced to the objectives via retronectin-coated plates (clontech) for 48-72 hours, and transduced cells were sorted by flow cytometer Aria III (BD Biosciences). For the production of lentivirus supernatants, HEK293T cells were transiently co-transfected with lentivirus vectors, psPAX2 and pMD2.G.

**Yeast two-hybrid screening**

Yeast two-hybrid screening was performed with the Matchmaker Gold Yeast Two-Hybrid System (Clontech). Human BAALC 1-6-8 cDNA was used as bait and cloned into the pGBKT7 vector in frame with the GAL4 DNA-binding domain (pBD-BAALC). Yeast Y2H GOLD cells were transformed with pBD-BAALC, subsequently mated to the purchased library strain transformed with a universal human cDNA library (Clontech cat. No. 630480). Interaction was confirmed as described in the Yeast Protocol Handbook (Clontech). After extraction of plasmids from positive clones, inserted cDNA was sequenced by 3130xL Genetic Analyzer (Applied Biosystems) and identical alignment was computationally searched by BLAST (Basic Local Alignment Search Tool, National Library of Medicine).

**Analysis of protein phosphorylation**

HEK293T cells were transiently transfected with 12 μg of pcDNA3-6xMYC-Mock or pcDNA3-6xMYC-BAALC vectors by PEI. Forty-eight hours after transfection, cells were serum-starved for 4 hours before stimulated by EGF at 10 ng/mL for 30 minutes, then harvested. After subsequent protein extraction, phosphorylated status of each cytoplasmic signaling (MAPK pathway, PI3K/AKT pathway, JAK/STAT pathway and NF-κB pathway)-related molecule was examined by immunoblot analysis.

## Immunoblotting

Cells were washed twice with ice cold PBS and harvested in protein lysis buffer [50 mM Tris (pH 7.4), 100 mM NaCl, 0.1 mM EDTA, 1 mM phenylmethylsulfonyl fluoride, 1 mM β-glycerophosphate, 2.5 mM sodium pyrophosphate, 1mM $Na_3VO_4$, 1x protease inhibitor (Roche) and PhosSTOP (Roche)]. Whole cell extracts were resolved by SDS-polyacrylamide gel electrophoresis (SDS-PAGE) and transferred onto polyvinylidene difluoride membranes. Membranes were probed with the following antibodies: anti-ERK, anti-phospho-ERK (Thr202/Tyr204), anti-MEKK1, anti-MKP3, anti-β-actin, anti-histone H3, anti-p90RSK, anti-phospho-p90RSK, anti-p38, anti-phospho-p38, anti-NF-κB, anti-phospho-NF-κB, anti-AKT, anti-phospho-AKT, anti-MYC-tag, anti-A-Raf, anti-phopho-A-Raf, anti-B-Raf, anti-phospho-B-Raf, anti-c-Raf, anti-phospho-c-Raf, anti-mTOR, anti-phospho-mTOR, anti-Raptor, anti-Rictor (Cell Signaling Technology), anti-JNK/SAPK1, anti-phospho- JNK/SAPK1, anti-JAK2, anti-phospho-JAK2, anti-STAT1, anti-phospho-STAT1, anti-STAT3, anti-phospho-STAT3, anti-STAT5, anti-phospho-STAT5, anti-STAT6, anti-phospho-STAT6 (BD pharmingen) and HRP-conjugated anti-FLAG-tag (Sigma

Aldrich) antibodies. For secondary antibodies, anti-rabbit IgG, or anti-mosue IgG, HRP-linked antibodies (Cell Signaling Technology) were used. Blots were detected using an ImmunoStar Zeta (Wako Pure Chemical Industries) and an LAS-3000 image analyzer (Fujifilm), as recommended by the manufacturers. Protein levels were quantified with ImageJ software (NIH). To obtain nuclear and cytoplasmic extracts, an Active Motif Nuclear Extract Kit was used according to the manufacturer's instructions.

**Co-immunoprecipitation (CoIP) assay**

pcDNA3-3xFLAG-KLF4, pcDNA3-6xMYC-Mock, pcDNA3-6xMYC-BAALC, pcDNA3-3xFLAG-MEKK1, pcDNA3-6xHis-MKP3, deletion mutants of 6xMYC-tagged BAALC, 3xFLAG tagged KLF4 and 3xFLAG-tagged MEKK1 were transiently transfected to HEK293T cells and cultured for 48 hours. Cells were lysed in cell lysis buffer, and the lysates were clarified by centrifugation. Cell extracts were pre-cleared with sepharose G protein beads (Sigma-Aldrich) at 4 ℃ for 1 hour, and then mixed with primary antibody (anti MYC-tag, anti HA-tag and anti FLAG-tag antibodies), rocked at 4 ℃ for over night. Immune complexes were immunoprecipitated by sepharose G protein beads next day. Beads were washed by Tris-Acetate-EDTA (TAE) buffer for 5 times. Bound proteins were eluted with hot SDS loading buffer and were resolved by SDS-PAGE, then protein-protein interaction was examined by immunoblotting.

**Time-lapse IP assay**

pcDNA3-6xMYC-Mock or pcDNA3-6xMYC-BAALC vectors were transiently transfected to HEK293T cells by PEI. Cells were starved for four hours, then stimulated by EGF at 10 ng/mL for indicated time (0 min, 15 min, 30 min, 60 min) just before ice-cold PBS wash x2, then lysed immediately in lysis buffer [50 mM Tris (pH 7.4), 100 mM NaCl, 0.1 mM EDTA, 1 mM phenylmethylsulfonyl fluoride, 1x protease inhibitor (Roche)]. Extracted proteins were immunoprecipitated by anti-MYC-tag antibody or anti-ERK antibody with sepharose G protein beads. Protein-protein interaction was examined by immunoblotting.

**In vitro pull-down assay**

pcDNA3-6xMYC-Mock, pcDNA3-6xMYC-BAALC, pcDNA3-6xHis-KLF4-Δ2 and pcDNA3-HA-MEKK1-Δ4 were transiently transfected to HEK293T cells and cultured for 48 hours before lysed. Expressed proteins were purified by c-MYC tagged Protein mild purification kit or His tagged Protein mild purification kit or HA tagged Protein mild purification kit (BML) according to the manufacturer's instructions. Purification efficiency was checked by coomassie brilliant blue stains. Samples were mixed in binding buffer (50 mM Tris-HCl, 250 mM NaCl, 0.05 % Nonidet P-40, 30 mM $MgCl_2$, pH 7.4) with protease inhibitor mixture (4 μg/mL) for 2 hours at 4 °C, then anti MYC-tag antibody was added before immunoprecipitation with sepharose G protein beads. Beads were washed by TAE buffer twice, then proteins bound to beads were resolved by SDS-PAGE. Protein-protein interaction was checked with immunoblotting.

**Cell culture**

HEK293T and Plat-A cells were cultured in DMEM-10 % heat inactivated FCS at

37 °C, 5 % $CO_2$. Human leukemia cell lines Kasumi-1, OCI-AML2, MV4-11 and HEL cells were cultured in RPMI1640-10% heat inactivated FCS at 37 °C, 5 % $CO_2$. Bone marrow cells of patient samples were maintained in RPMI1640 plus 20 % heat inactivated FCS supplemented with cytokines of IL-3, hSCF, FLT3L and MGDF (Wako Pure Chemical Industries) at 100 ng/mL.

**Cell growth curve**

To assess cell proliferation, $1 \times 10^5$ cells of AML cell lines and human primary bone marrow cells were counted and transferred to 6-well plate with 4mL medium. Cell number was counted every other day.

**Real-time quantitative PCR (qRT-PCR).**

Total RNA was isolated with RNeasy mini kit (Qiagen) and reverse transcribed with Reverse script kit (TOYOBO) to generate cDNA. Real-time quantitative polymerase chain reaction (PCR) was carried out with LightCycler480 (Roche) according to the manufacturer's instructions. The results were normalized to GAPDH levels. Relative expression levels were calculated using the 2-ΔΔCt method. Primers used for qRT-PCR were listed in Table 1.

**siRNA interference**

Specific shRNAs targeting human BAALC were designed and cloned into pSIREN-RetroQ-ZsGreen vectors (Clontech). Control shRNA is a nonfunctional construct targeting luciferase (sh_*Luc.*). The target sequences were provided in Table 2.

**Immunofluorescence assay**

For Kasumi-1 cells, a total of $1 \times 10^4$ to $5 \times 10^4$ cells were cytospun onto glass slides. The cells were fixed with 3.7 % formaldehyde in PBS for 30 minutes, permeabilized by 0.2 % Triton X in PBS for 10 minutes, and blocked with 1 % BSA in PBS for 60 minutes. Then, the slides were incubated with rabbit anti–KLF4 antibody (1:100 dilution; Cell Signaling Technology) overnight at 4 °C, followed by incubation with Alexa Fluor 594 goat anti-rabbit IgG (1:250 dilution; Invitrogen) and DAPI (1:1,000 dilution; Invitrogen) for 90 minutes. Cells were gently washed by PBS, then they were treated with ProLong Gold Antifade Reagent (Invitrogen). Images were acquired using an Olympus FluoView FV10i confocal microscope with a × 60 objective oil immersion lens. For HEK293T cells, a total of $1 \times 10^4$ to $5 \times 10^4$ cells were cultured on glass slides transiently transfected with pcDNA3-3xFLAG-KLF4 and pcDNA3-6xMYC-BAALC or Mock vectors before fixation and permeabilization. Each slide was incubated with rabbit anti–KLF4 antibody (1:100 dilution; Cell Signaling Technology) or mouse anti-MYC-tag antibody (1:100 dilution; Cell Signaling Technology), followed by incubation with Alexa Fluor 647 goat anti-rabbit IgG (1:250 dilution; Invitrogen) or Alexa Fluor 488 goat anti-mouse IgG (1:250 dilution; Invitrogen) and DAPI (1:1,000 dilution).

**Cell cycle and apoptosis assay**

For cell cycle analysis, cells were fixed with fixation buffer and permeabilized with permeabilization wash buffer (BioLegend) before incubated in PBS with 3 % heat inactivated FCS, DAPI 1:1000 and 100 μg/mL RNAseA until flow cytometry analysis.

For apoptosis assay, cell apoptosis was determined by Annexin V Apoptosis Detection Kit APC (eBioscience Inc.). Approximately $2 \times 10^5$ cells from each experimental group were washed with PBS and then suspended by annexin-binding buffer. Subsequently, 5 uL annexin V was added to each sample. Incubated for another 30 min, the cells were diluted by buffer and stained with DAPI just before analyzed with flow cytometry.

**Flow cytometry**

Isolation of $CD34^+/CD38^-$ fraction from human normal or leukemic bone cells and isolation of leukemia cell lines transduced with immunofluorescent color markes of GFP, Kusabira-Orange and Venus were performed using FACSAria III (BD) cell sorter. For isolation of $CD34^+/CD38^-$ fraction from human primary bone marrow cells, FITC-conjugated anti-human CD34, and PE-conjugated anti-human CD38 antibodies were used (eBioscience). For checking monocytic differentiation state of leukemia cells, Biotin-conjugated anti-human CD11b or CD14 and Streptavidin-APC (eBioscience) were used. Analysis was performed using FlowJo software (Tree Star

Inc.).

**IC50 evaluation**

AML cell lines were grown in RPMI 1640 plus 10 % heat inactivated FCS. For the growth inhibition assay, cells were placed at a density of $1 \times 10^5$ cells/mL. Different concentrations of U0126 were added to the media. Cell viability was assessed by counting the number of trypan blue excluding cells 4 days after starting culture. The doses that inhibited 50 % proliferation were analyzed by the median-effect method[34].

**Xenograft mouse model**

A xenograft mouse model of human AML with high expression of BAALC was developed using NSG mice. Before transplantation, NSG mouse was treated with i.p. injection of cyclophosphamide 100 mg/kg/day for 2 days. At day 0 and day 1, $5 \times 10^6$ cells/body of Kasumi-1 cells transduced with indicated viruses were i.v. injected. Peripheral blood (PB) was collected twice a week and chimerism was checked by flow cytometer. Once PB chimerism of leukemia cells exceeded 1 %, treatment either by

U0126 (25 μmol/kg/week i.p.) or doxycycline (diluted in drinking water at 1 g/L+3 % sucrose) was started.

**Statistics**

Statistical significance of differences between groups was assessed with a 2-tailed unpaired Student's t test. Equality of variances in two populations was calculated with F-test. Differences were considered statistically significant at a P value of less than 0.05. In leukemia cell transplantation experiments, the overall survival of mice is depicted by a Kaplan-Meier curve. Survival between groups was compared using the log-rank test. To measure the correlation between *BAALC* mRNA expression and sensitivity to MEK inhibitor (U0126) in human AML cell lines and patients samples, the Spearman's rank correlation coefficient was used.

**Study approval**

BM cells derived from 80 patients with AML were obtained from the Department of Hematology and Oncology of the University of Tokyo Hospital. Seven bone marrow cells from patients diagnosed with lymphoid neoplasia without bone marrow invasion were used as normal controls. The study was approved by the ethics committee of the University of Tokyo, and written informed consents were obtained from all patients whose samples were collected.

## Results

### BAALC promotes leukemia cell expansion.

We first examined the expression levels of *BAALC* in CD34+ CD38- fraction of primary human bone marrow samples from control subjects and AML patients and in four AML cell lines. CD34+ CD38- AML cells showed five-fold higher *BAALC* than control subjects (Figure 1).

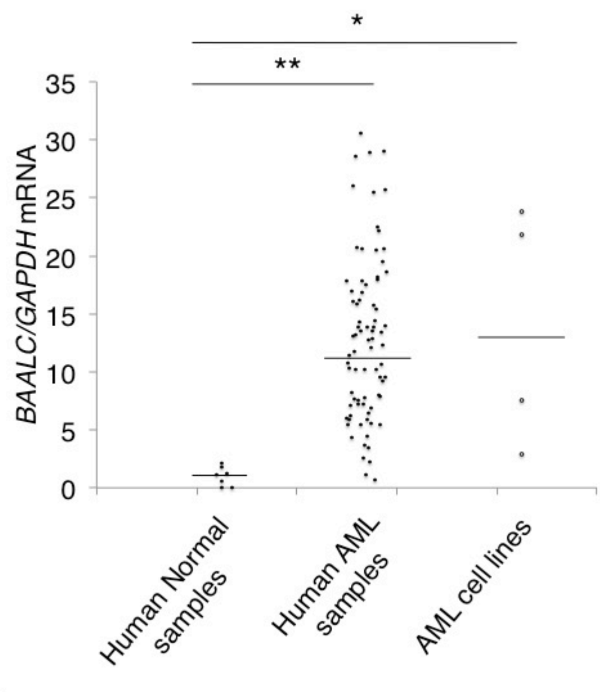


**Figure 1. Comparison of *BAALC* expressions in human bone marrow cells and AML cell lines.**

Relative *BAALC* expressions in primary human bone marrow cells from AML patients (n = 80), control subjects (n = 7) and AML cell lines (n = 4). Values are normalized to *BAALC* expression in control subjects.

Data are mean ± SEM values. * $P < 0.05$, ** $P < 0.01$.

*BAALC* was higher even in human primitive $CD34^+$ $CD38^-$ AML cells compared to normal $CD34^+$ $CD38^-$ cells which are rich in hematopoietic progenitor cells (Figure 2).

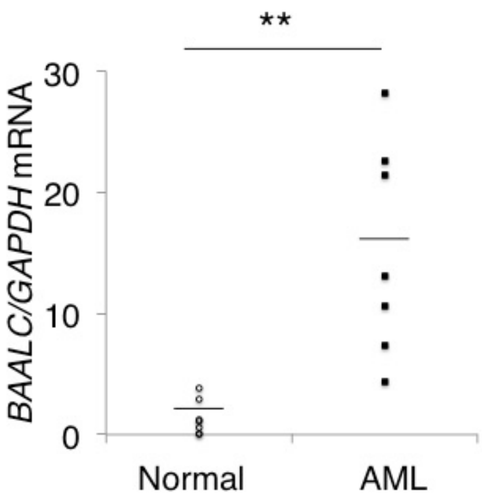


**Figure 2. Comparison of *BAALC* expressions in immature fraction of human bone marrow cells from AML patients and control subjects.**

Relative *BAALC* expressions in $CD34^+$ $CD38^-$ fraction of primary human bone marrow cells from AML patients (n = 7), control subjects (n = 7). Values are normalized to *BAALC* expression in primary human whole bone marrow cells from control subjects. Data are mean ± SEM values. ** $P < 0.01$.

Taken into account that high BAALC expression represents cases belonging to the upper quartile of BAALC expression in a cohort of AML patients[9], among four AML cell lines, Kasumi-1 and OCI-AML2 showed comparable *BAALC* levels as BAALC-high AML patient samples, while *BAALC* expressions were low in HEL and MV4-11. From this finding, hereafter we used Kasumi-1 as BAALC-high leukemia cells and HEL as BAALC-low cells (Figure 3A and 3B).

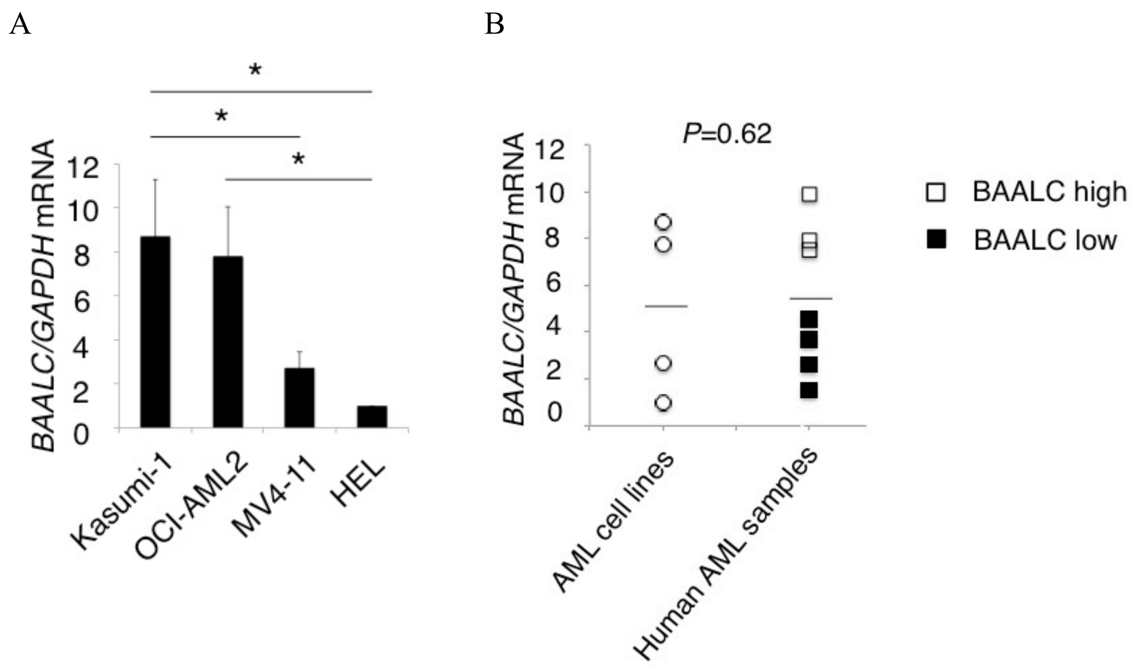


**Figure 3. Comparison of *BAALC* expressions in AML cell lines and immature fraction of human bone marrow cells.**

(A) Relative BAALC expressions in AML cell lines (n = 4). Values are normalized to BAALC expression in HEL cells. (B) Comparison of Relative BAALC expressions between CD34+CD38- primary AML cells (n = 7) and AML cell lines (n = 4). Values are normalized to BAALC expression in HEL cells. Data are mean ± SEM values. * P < 0.05.

When full-length of BAALC (1-6-8 form) was lentivirally transduced to HEL (Figure 4A), they showed an increased proliferative capacity (Figure 4B) and accelerated cell cycle progression (Figure 4C and 4D), while apoptotic status was not altered (Figure 4E and 4F).

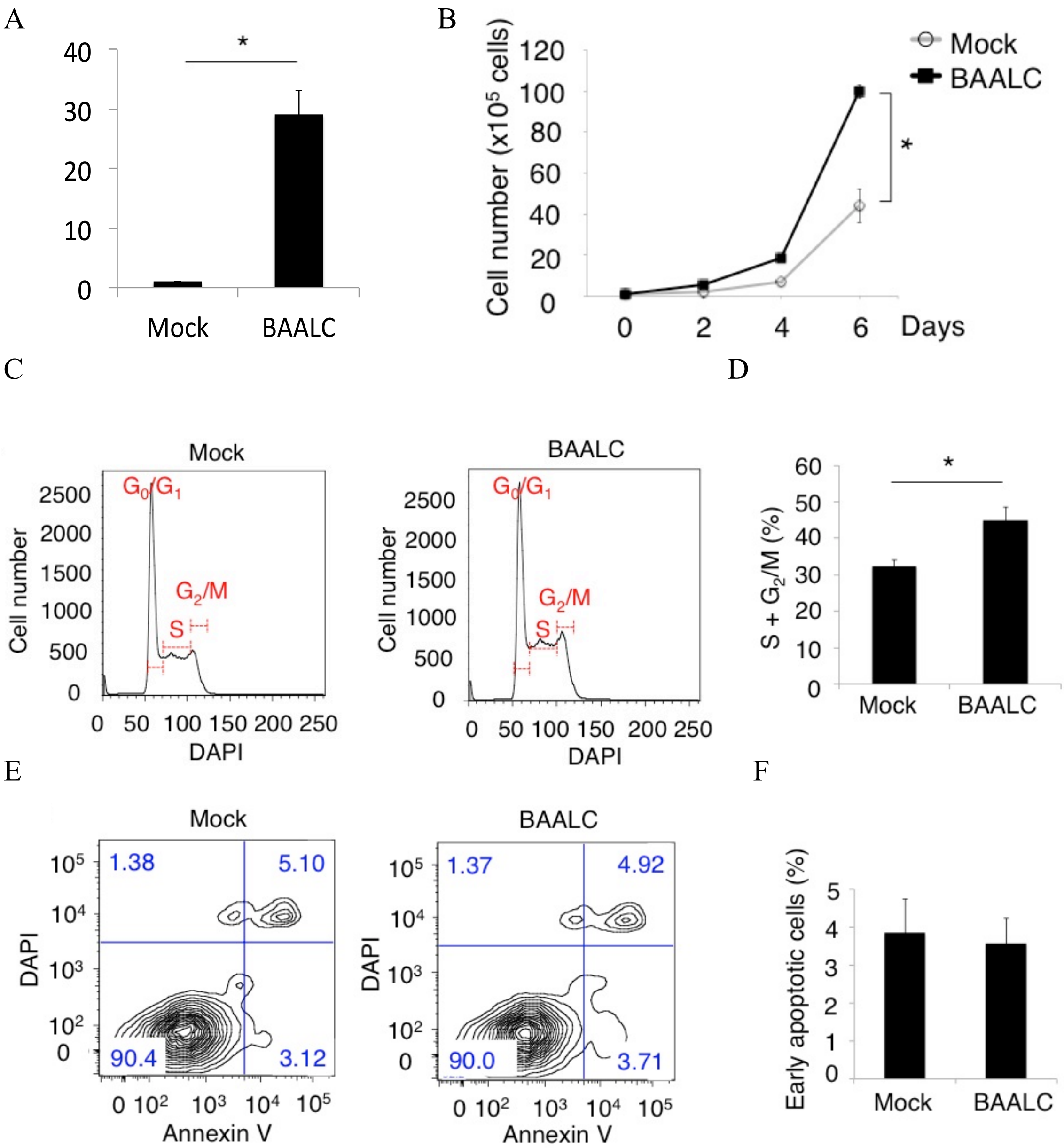


**Figure 4. Overexpression of BAALC promotes proliferation of HEL cells.**

(A) Relative *BAALC* expressions in HEL cells transduced with BAALC or control vector. Values are normalized to *BAALC* expression in HEL cells transduced with control vector. (n = 3) (B) Growth curve of HEL cells transduced with BAALC or control vector (mock). (n = 3) (C and D) Cell cycle was assessed with flow cytometry in HEL cells transduced with BAALC or control vector. (C) Representative flow cytometric data showing cell cycle distributions. (D) Cumulative data showing percentage of S and G2/M phase (n = 3). (E and F) Apoptotic status in HEL cells transduced with BAALC or control vector. (E) Representative flow cytometric data of Annexin V and DAPI staining. (F) Cumulative data of the frequency of early apoptotic cells (Annexin $V^+$ $DAPI^-$) (n = 3). Data are mean ± SEM values. * P < 0.05.

On the other hand, knockdown of BAALC using retroviral short hairpin RNA (shRNA) in Kasumi-1 cells (Figure 5A) partially blocked proliferation (Figure 5B) and cell cycle progression (Figure 5C and Figure 5D) without any effects on apoptosis (Figure 5E and 5F).

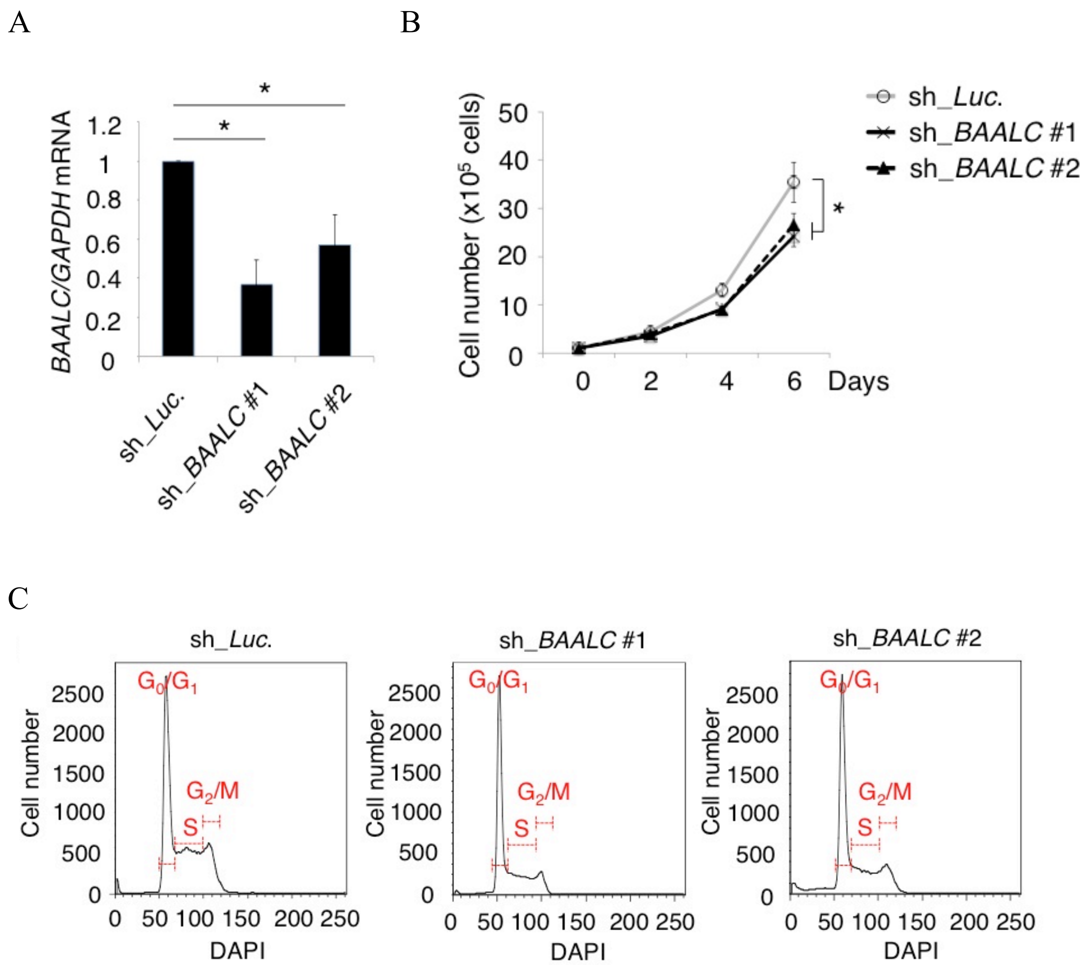

D

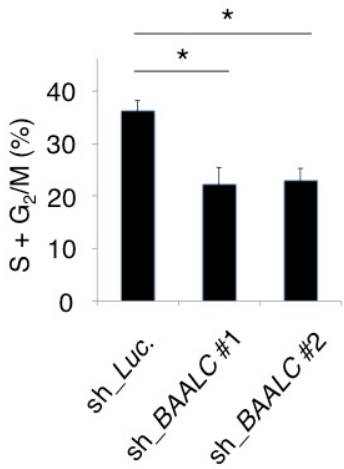


F

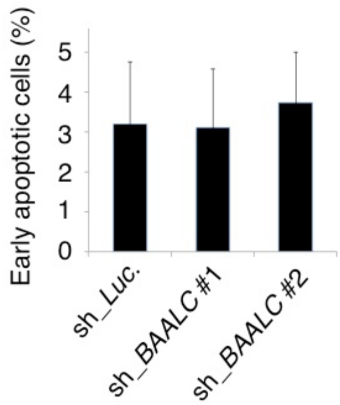


E

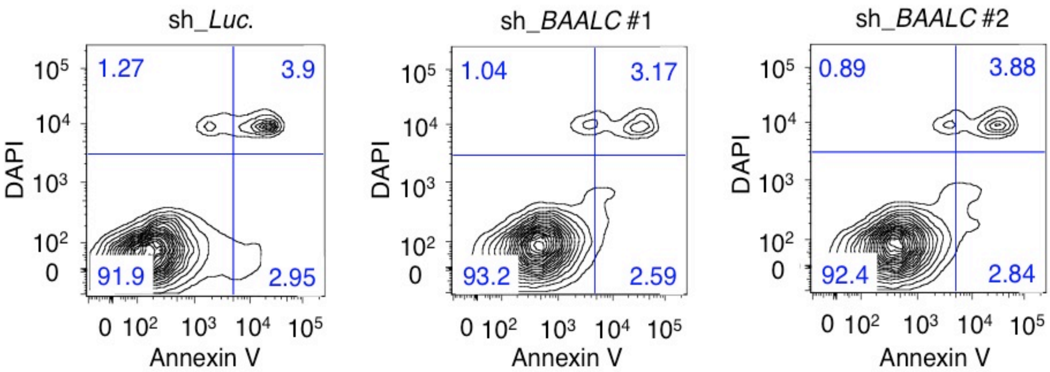


**Figure 5. Knockdown of BAALC suppresses proliferation of Kasumi-1 cells.**

(A) Relative BAALC expressions in Kasumi-1 cells transduced with control (sh_*Luc.*) or BAALC (sh_*BAALC*) shRNA (n = 3). Values are normalized to BAALC expression in control shRNA-transduced cells. (B) Growth curve of Kasumi-1 cells transduced with sh_*Luc*. or sh_*BAALC* (n = 3). (C and D) Cell cycle was assessed with flow cytometry in Kasumi-1 cells transduced with sh_*Luc*. or sh_*BAALC*. (C) Representative flow cytometric data showing cell cycle distributions. (D) Cumulative data showing percentage of S and G2/M phase (n = 3) (E and F) Apoptotic status in Kasumi-1 cells transduced with sh_*Luc*. or sh_*BAALC*. (E) Representative flow cytometric data for Annexin V and DAPI staining. (F) Cumulative data of the frequency of early apoptotic cells (Annexin $V^+$ $DAPI^-$) (n = 3). Data are mean ± SEM values. * $P < 0.05$.

Knockdown of BAALC in Kasumi-1 cells also promoted monocytic differentiation as exemplified by higher expressions of differentiation-associated markers such as CD11b and CD14 than those of control cells (Figure 6A and Figure 6B). These results indicate that BAALC promotes proliferation, cell cycle progression of leukemia cells along with inhibition of leukemia cell differentiation.

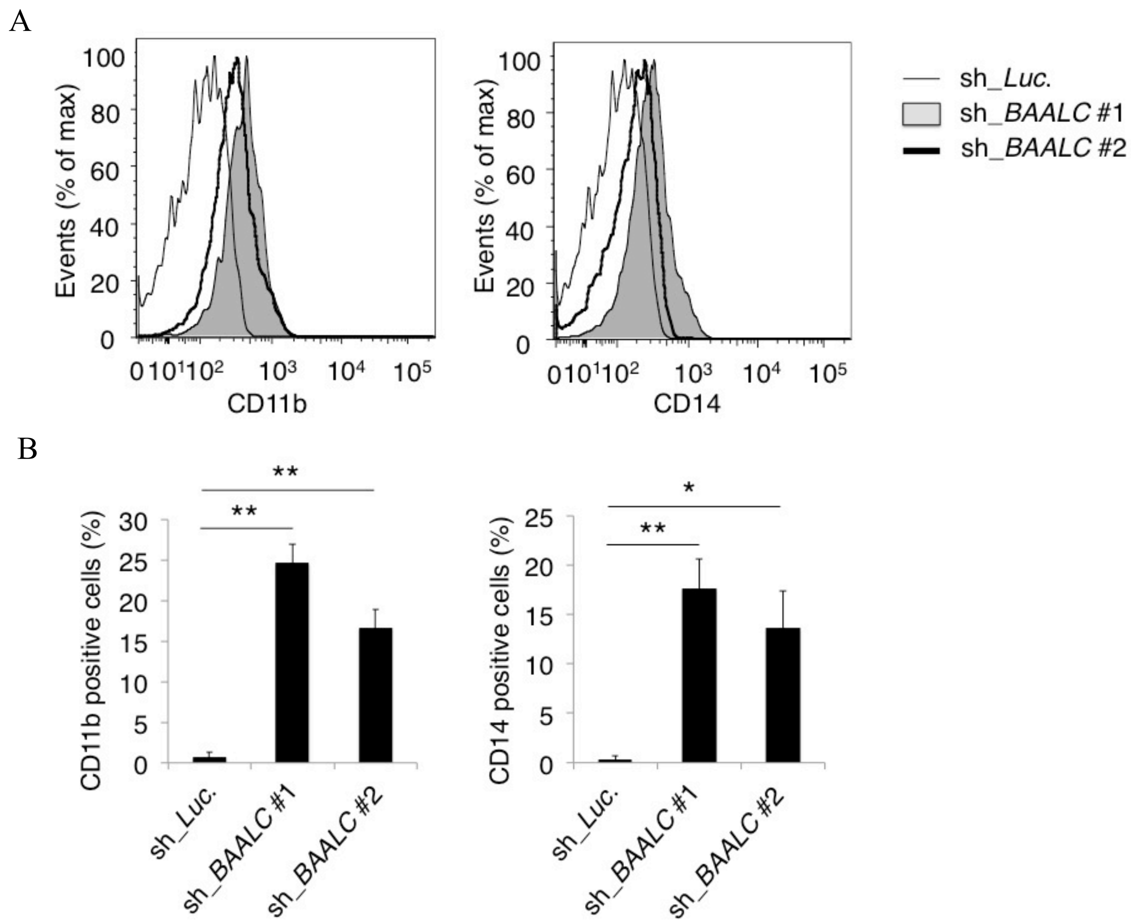


**Figure 6. Knockdown of BAALC promotes monocytic differentiation of Kasumi-1 cells.** (A) Representative flow cytometric data showing CD11b and CD14 expressions in sh_*Luc*. or sh_*BAALC*-transduced Kasumi-1 cells. (B) Cumulative data of CD11b or CD14 positive cells (n = 3). Data are mean ± SEM values. * P < 0.05, ** P < 0.01.

**MEKK1 and KLF4 are novel interacting partners of BAALC.**

To gain insight into molecular functions of BAALC, interacting partners of BAALC were explored with a yeast two-hybrid system on a proteome-wide scale (Figure 7A). Using BAALC as bait and a cDNA library from adult human tissues as prey, we identified eight possible interacting molecules (Figure 7B).

A

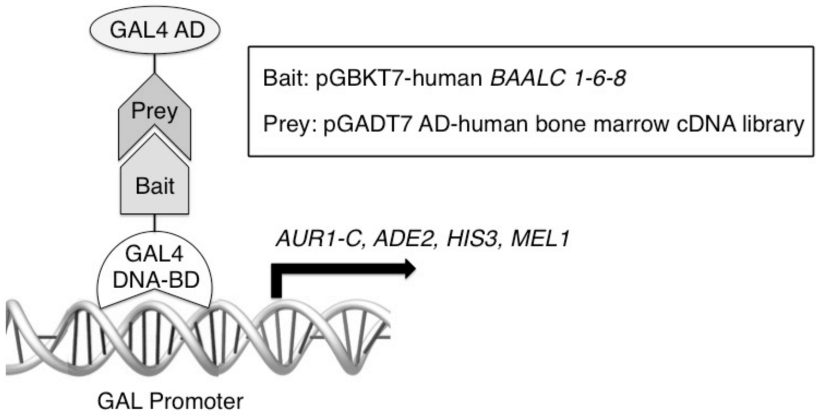


B

Two-hybrid Result

#1; Mitogen-activated protein kinase kinase kinase 1 (MEKK1, MAP3K1)
#2; Kruppel-like factor 4 (KLF4)
#3; ATPase, Na+/K+ transporting, beta 3 polypeptide (ATP1B3)
#4; Ring finger protein 2 (RNF2)
#5; Chromodomain helicase DNA binding protein 1-like (CHD1L)
#6; Cyclin-dependent kinase 2 interacting protein (CINP)
#7; Oxysterol binding protein-like 1A (OSBPL1A)
#8; Adaptor-related protein complex 1, gamma 1 subunit (AP1G1)

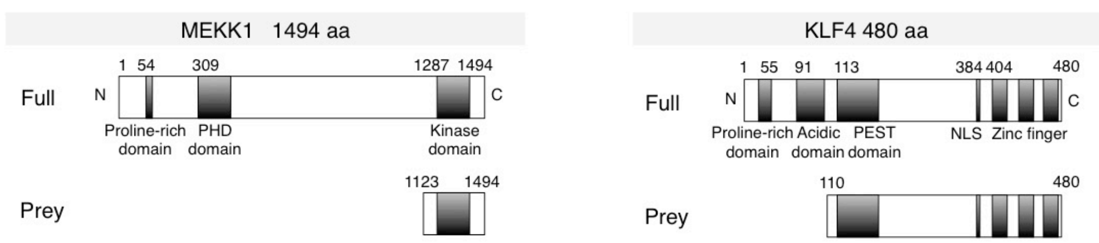

**Figure 7. Screening binding partners of BAALC by yeast two-hybrid method.**
(A) Schematic abstract of yeast two-hybrid screening. Human BAALC 1-6-8 was used as bait and a cDNA library from adult human tissues as prey. (B) Potential binding partners of BAALC detected by yeast two-hybrid screening. Coded sequences contained in prey vectors were shown for MEKK1 and KLF4.

Among them, we focused on MEKK1 and KLF4, both of which are known to have substantial roles in Ras/Raf/MEK/ERK pathway, one of pivotal oncogenic signaling cascades in AML[19, 35]. MEKK1 works as a scaffold protein as well as a kinase in MAPK cascade, and specifically potentiates ERK pathway by recruiting Raf, MEK and ERK[19]. KLF4 is a downstream target of ERK, regulated by direct interaction [35]. To validate the interactions between BAALC and MEKK1 or KLF4, we performed co-immunoprecipitation (CoIP) assay in HEK293T cells. Intriguingly, BAALC bound to MEKK1 more tightly in the presence of epidermal growth factor (EGF), a potent ERK activator (Figure 8A and 8B).

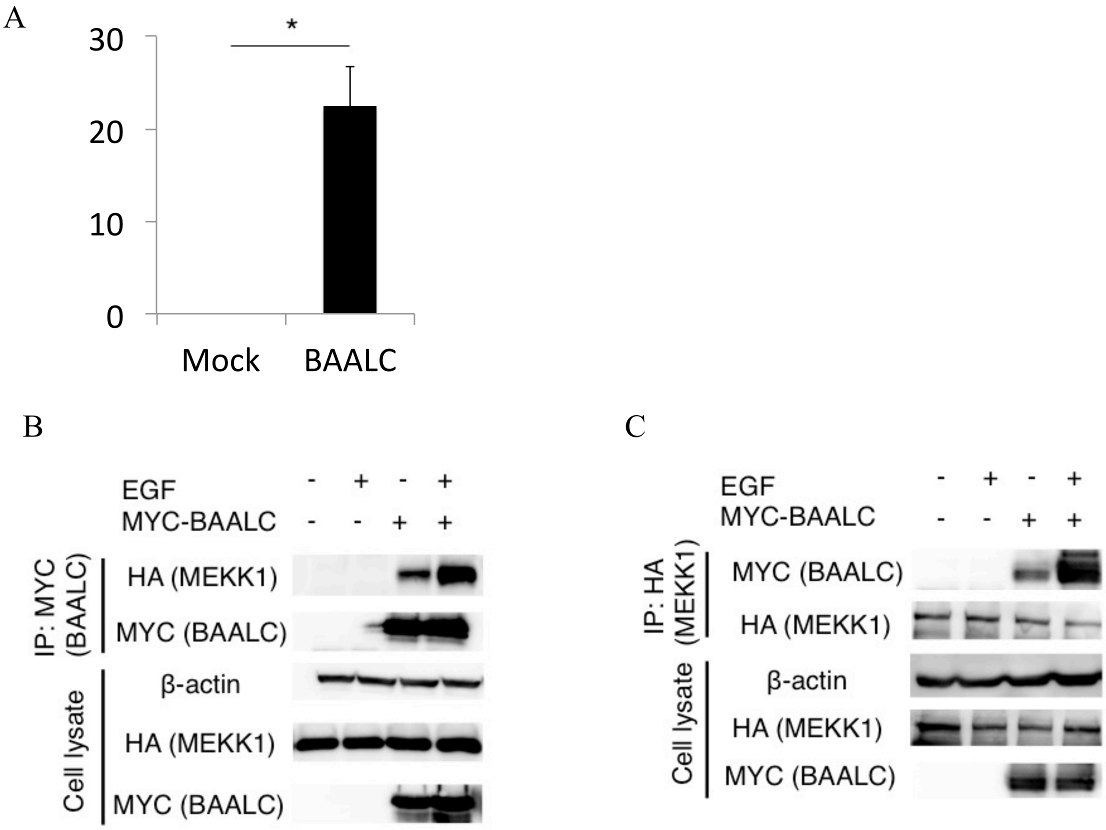


**Figure 8. BAALC interacts with MEKK1 stimulation dependently.**

(A) Relative *BAALC* expressions in HEK293T cells transiently transfected with BAALC or control vector. Values are normalized to *BAALC* expression in HEL cells transduced with control vector. (n = 3)

(B and C) Interaction between BAALC and MEKK1 was examined by co-immunoprecipitation assay. HEK293T cells were co-transfected with His-tagged MEKK1 and MYC-tagged BAALC. Cells were stimulated by EGF (10 ng/mL) or dimethyl sulfoxide (DMSO) for 30 minutes, and immunoprecipitated by anti-MYC tag antibody followed by blotting with anti-HA tag antibody (B) or immunoprecipitated by anti-HA tag antibody followed by blotting with anti-MYC tag antibody (C).

On the other hand, BAALC-KLF4 complex was formed independently of stimulation (Figure 9A and 9B).

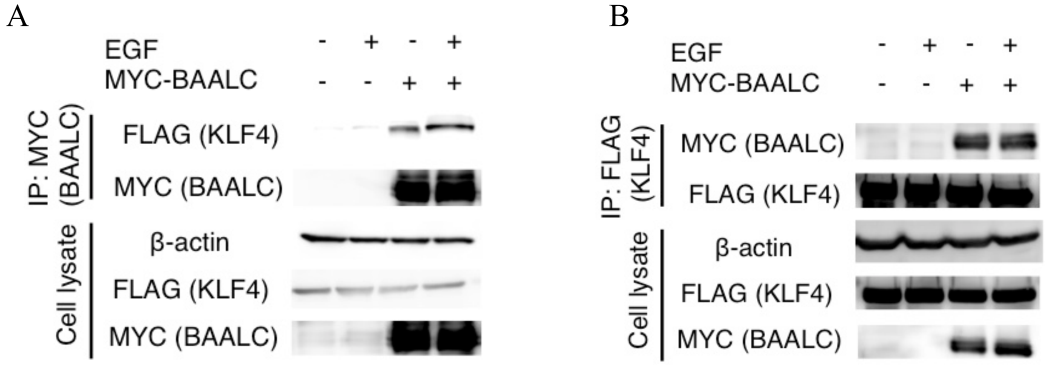


**Figure 9. BAALC interacts with KLF4 stimulation independently.**

Interaction between BAALC and KLF4 was examined by co-immunoprecipitation assay. HEK293T cells were cotransfected with FLAG-tagged KLF4 and MYC-tagged BAALC. Cells stimulated by EGF were immunoprecipitated by anti-MYC tag antibody followed by blotting with anti-FLAG tag antibody (A) or immunoprecipitated by anti-FLAG tag antibody followed by blotting with anti-MYC tag antibody (B).

Protein-protein interactions between BAALC and MEKK1 or KLF4 were further affirmed by in vitro pull-down assays using purified proteins obtained from mammalian cells (Figure 10A and 10B).

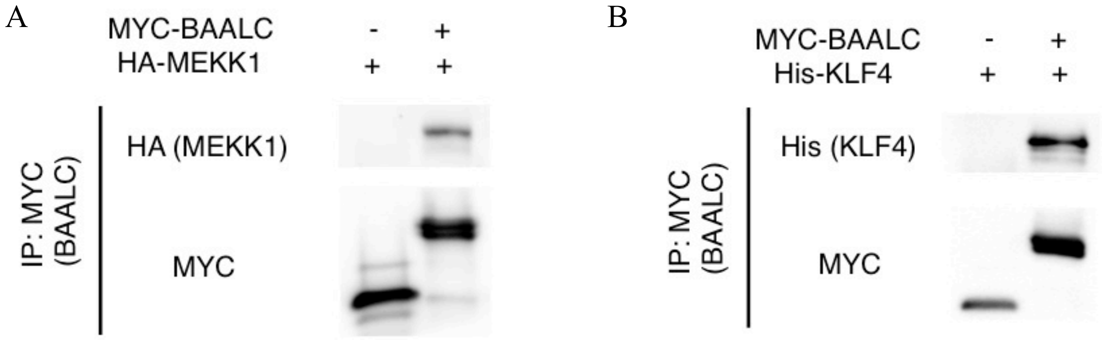

**Figure 10. Direct interaction of BAALC with MEKK1 and KLF4 is confirmed by in vitro pull-down assay.**

(A) Interaction between BAALC and MEKK1 was assessed by in vitro pull-down assay. To obtain soluble recombinant protein, shortened form of MEKK1 (MEKK1-Δ4) was utilized (see Figure 12). Purified MYC-tagged BAALC and HA-tagged MEKK1-Δ4proteins were mixed and immunoprecipitated by anti-MYC tag antibody followed by blotting with anti-HA tag antibody. (B) Interaction between BAALC and KLF4 by in vitro pull-down assay. To obtain soluble recombinant protein, shortened form of KLF4 (KLF4-Δ2) was utilized (see Figure 12). Purified MYC-tagged BAALC and His-tagged KLF4-Δ2 proteins were mixed and immunoprecipitated by anti-MYC tag antibody followed by blotting with anti-His tag antibody.

These results illustrate that BAALC directly interact with MEKK1 in a stimulation-dependent, and with KLF4 in a stimulation-independent manner.

**N-terminal region of BAALC is necessary and sufficient for the interactions with MEKK1 and KLF4.**

Next, we elucidated an essential binding region of each protein using a series of deletion mutants of BAALC, MEKK1 and KLF4. CoIP assay revealed that N-terminal region of BAALC (amino acids 1-35) was an indispensable prerequisite for its binding to MEKK1 and KLF4 (Figure 11A and 11B).

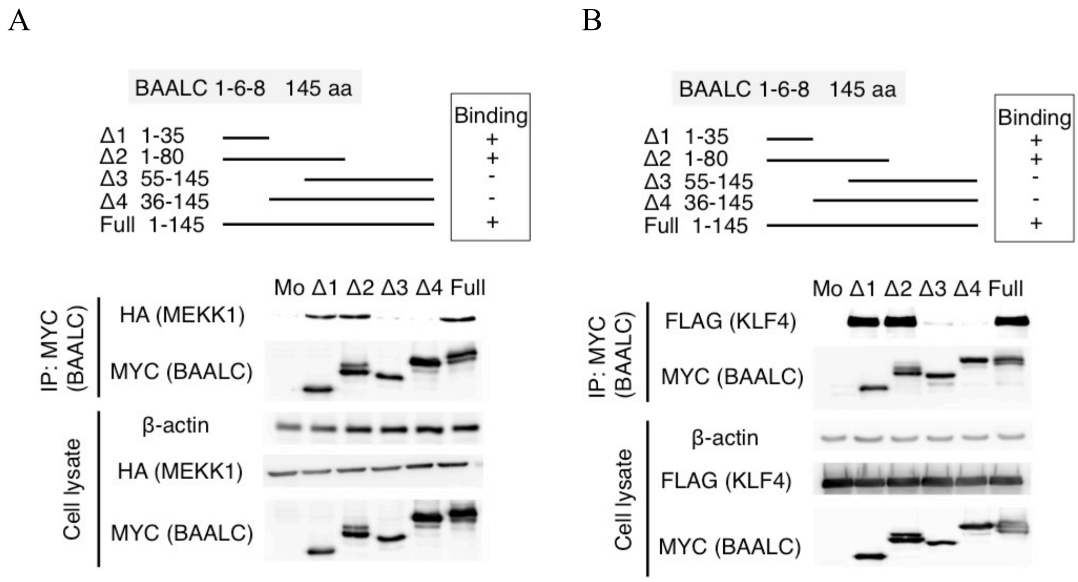


**Figure11. N-terminal region of BAALC interacts with MEKK1 and KLF4.**

(A) The binding site of BAALC with MEKK1. HA-tagged MEKK1 and MYC-tagged deletion mutants of human BAALC were cotransfected into HEK293T cells. Immune complexes were precipitated by anti-MYC tag antibody and blotted by anti-HA tag antibody. (B) The binding site of BAALC with KLF4. FLAG-tagged KLF4 and MYC-tagged deletion mutants of BAALC were cotransfected into HEK293T cells. Immune complexes were precipitated by anti-MYC tag antibody and blotted by anti-FLAG tag antibody.

Notably, this N-terminal region of BAALC is conserved across all mammals expressing BAALC, indicating the functional importance of this region[10, 36]. HEL cells expressing deletion mutants of BAALC harboring N-terminal 1-35 amino acid sequence (Δ1, Δ2) showed comparable proliferation (Figure 12A) and cell cycle progression (Figure 12B and 12C) to cells expressing full-length BAALC. By contrast, BAALC mutants lacking N-terminal domain (Δ3, Δ4) had no effect on proliferation and cell cycle progression, underscoring a fundamental role of this region for proliferative capacity of BAALC.

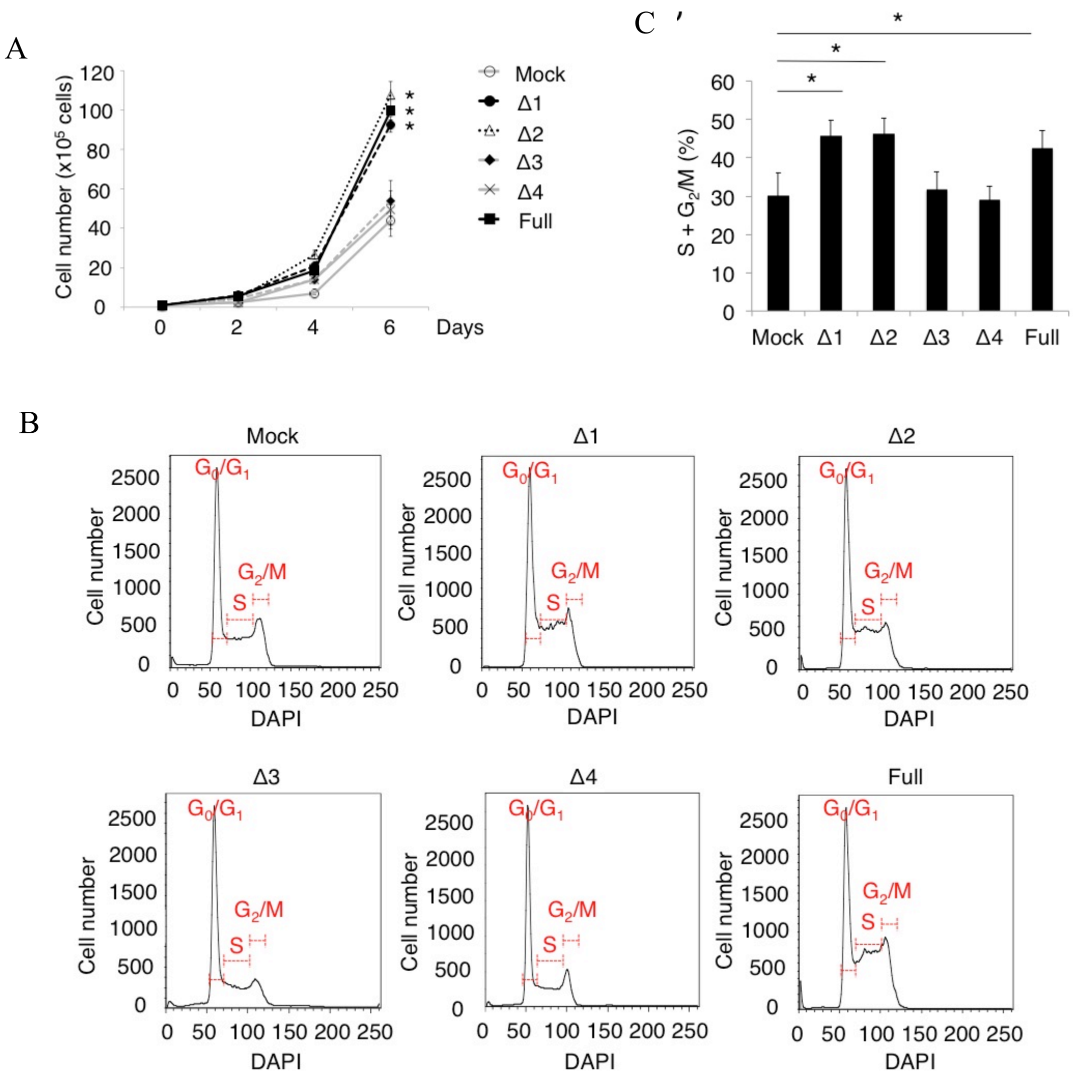


Figure 12. **N-terminal region of BAALC is necessary and sufficient for leukemogenic function of BAALC.**

(A) Growth curve of HEL cells transduced with a series of deletion mutants of BAALC. Comparison was made between each BAALC-expressing cells and mock-transduced cells (n = 3). (B and C) Cell cycle was assessed by flow cytometry in HEL cells transduced with each deletion mutant of BAALC. (B) Representative flow cytometric data showing cell cycle

distributions. (C) Cumulative data showing % of cells in S and $G_2$/M phase (n = 3).
Data are mean ± SEM values. * P < 0.05.

Furthermore, it was found that C-terminal region of MEKK1 and KLF4 were necessary for their interactions with BAALC (Figure 13A and 13B).

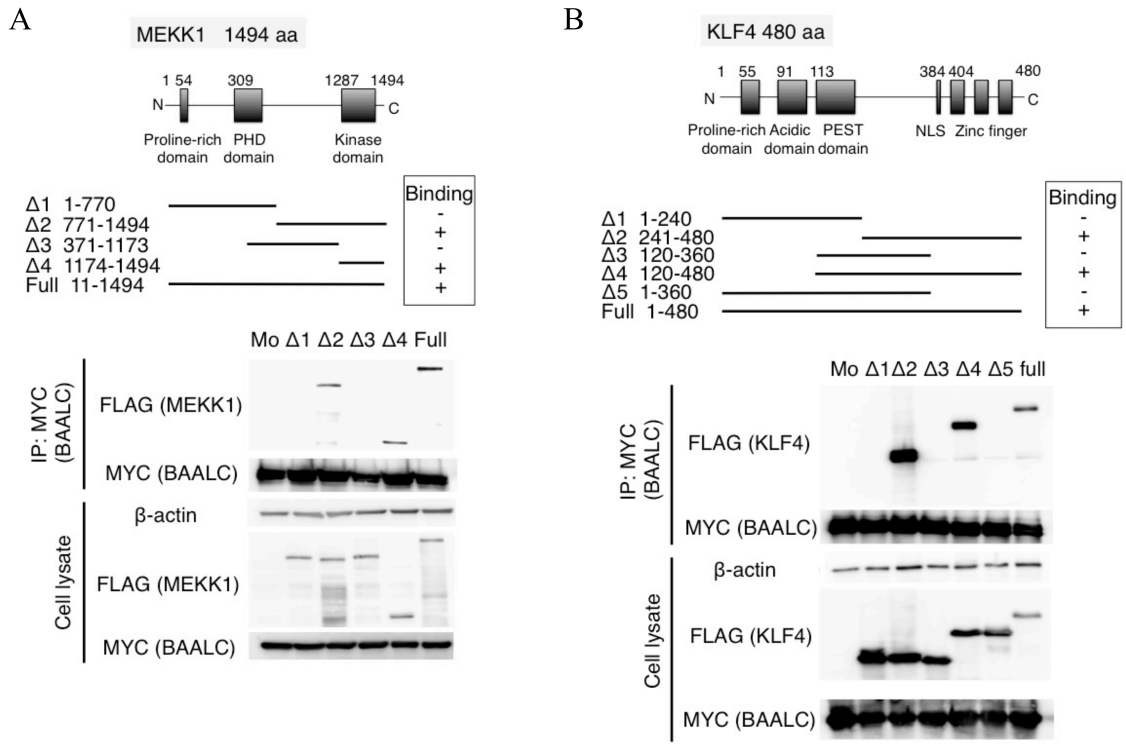


**Figure 13. Binding sites in MEKK1 and KLF4 for BAALC**

(A) The binding site in MEKK1 for BAALC determined by CoIP assay. MYC-tagged BAALC and FLAG-tagged deletion mutants of MEKK1 were cotransfected into HEK293T cells. Immune complexes were precipitated by anti-MYC-tag antibody and blotted by anti-FLAG tag antibody. (B) The binding site in KLF4 for BAALC determined by CoIP assay. MYC-tagged BAALC and FLAG-tagged deletion mutants of KLF4 were cotransfected into HEK293T cells. Immune complexes were precipitated by anti-MYC-tag antibody and blotted by anti-FLAG tag antibody.

MEKK1 has a kinase domain in its C-terminus and MEK1 interacts with this region[37], suggesting that BAALC possibly modifies ERK pathway through interacting with C-terminus of MEKK1 and alter the docking of signaling molecules around MEKK1. Since KLF4 has a nuclear localization signal (NLS) motif in its C-terminus[38], it is supposed that BAALC might affect nuclear localization of KLF4. These findings indicate that the N-terminal region of BAALC is essential for cell cycle progression and inhibiting differentiation of myeloid leukemia cells through interactions with C-terminal regions of MEKK1 and KLF4.

**BAALC prolongs ERK activation by inhibiting reassociation of an ERK-specific phosphatase MKP3.**

Considering that MEKK1 and KLF4 are both involved in ERK pathway[19, 35], we postulated that BAALC induces leukemia cell proliferation by potentiating MEK/ERK signaling. Using BAALC-overexpressing HEK293T cells, we found that BAALC specifically up-regulated the activities of ERK and its direct downstream target ribosomal protein S6 kinase, 90kDa (p90RSK)[39], without affecting the phosphorylation status of other upstream molecules of ERK (Figure 14A). The activities of other signaling pathways including PI3K-AKT, JAK-STAT, NF-κB pathways were not altered by BAALC (Figure 14B), suggesting BAALC specifically affects the activity of ERK.

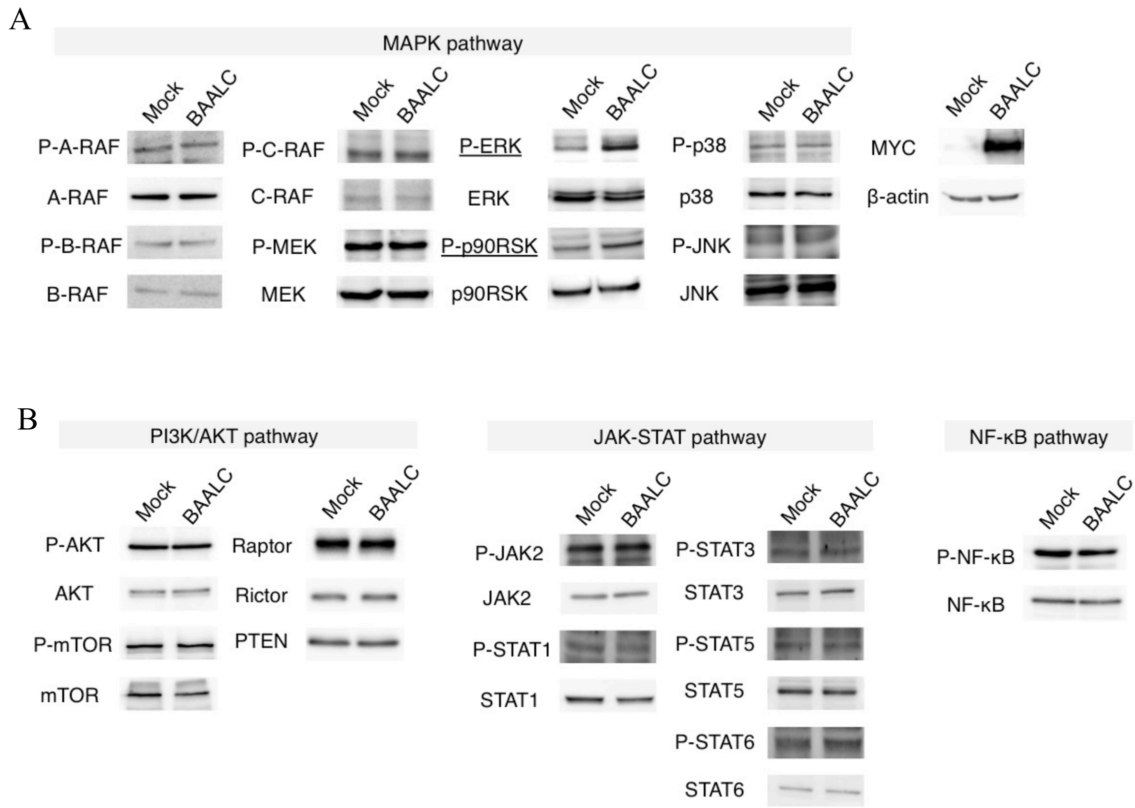


**Figure 14. Screening phosphorylation status of cytoplasmic signal transduction-related molecules.**

(A) Immunoblotting of phosphorylated proteins of MAPK signaling cascade in HEK293T cells transfected with MYC-tagged BAALC or control vector. Cells were stimulated with EGF (10 ng/mL) for 30 minutes. (B) Immunoblotting of phosphorylated proteins of PI3K/AKT, JAK-STAT and NF-κB pathways.

Similarly, HEL cells transduced with BAALC showed prolonged ERK activation compared to the control cells (Figure 15A), while knockdown of BAALC decreased the ERK activation in Kasumi-1 cells (Fig. 15B).

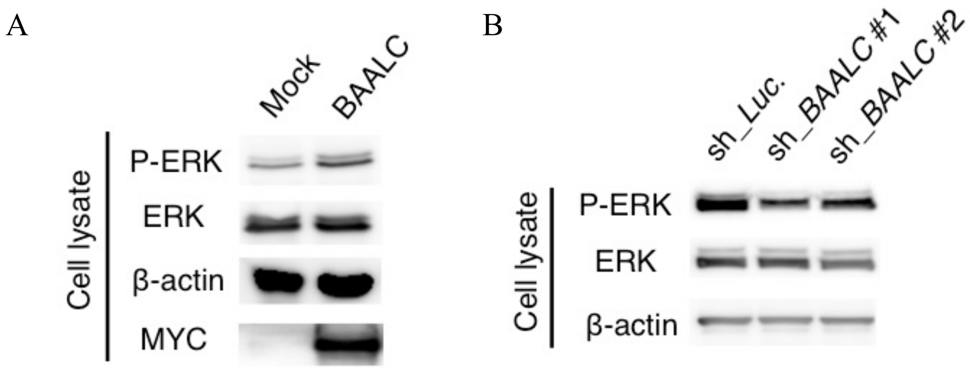


**Figure 15. BAALC up-regulates activity of ERK pathway.**

(A) Immunoblotting of phosphorylated ERK in HEL cells transduced with MYC-tagged BAALC. Cells were stimulated with PMA (100 ng/mL) for 6 hours. (B) Immunoblotting of phosphorylated ERK in Kasumi-1 cells transduced with sh_BAALC or sh_Luc. Cells were stimulated with PMA (100 ng/mL) for 6 hours.

A time lapse analysis of ERK phosphorylation after phorbol myristate acetate (PMA) treatment revealed that not a maximal intensity but a duration of ERK activation was affected by BAALC in HEL cells (Figure 16).

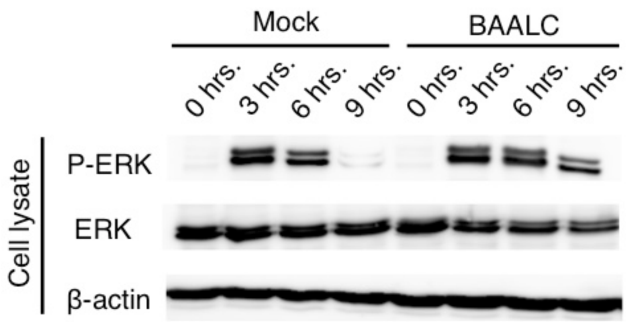


**Figure 16. BAALC induces prolonged up-regulation of ERK pathway.**
Immunoblotting of phosphorylated ERK in HEL cells transduced with BAALC. Cells were stimulated with PMA (100 ng/mL) for the indicated time periods.

As shown above, BAALC potentiated ERK phosphorylation without influencing kinase activity in the upstream of ERK, although it has no known kinase or phosphatase sequence motifs[14]. In addition, MEKK1 scaffolds components of its own signaling cascade, and thus positional relationship of these molecules around MEKK1 are fundamental in efficient ERK activation. These facts made us hypothesize that BAALC contribute to the sustained ERK phosphorylation by hindering the interaction between ERK and mitogen-activated protein kinase phosphatase 3 (MKP3/ DUSP6 dual specificity phosphatase 6), an ERK-specific phosphatase which mediates deactivation of ERK signaling[40]. To test this hypothesis, we conducted a time lapse analysis of CoIP assay, in which HEK293T cells transiently overexpressing BAALC were harvested at the indicated time points after stimulation with EGF and analyzed for the interaction between BAALC, ERK, MKP3 and MEKK1. BAALC bound to MEKK1 immediately after EGF stimulation, strongest at around 30 minutes after stimulation (Figure 17A and 17B).

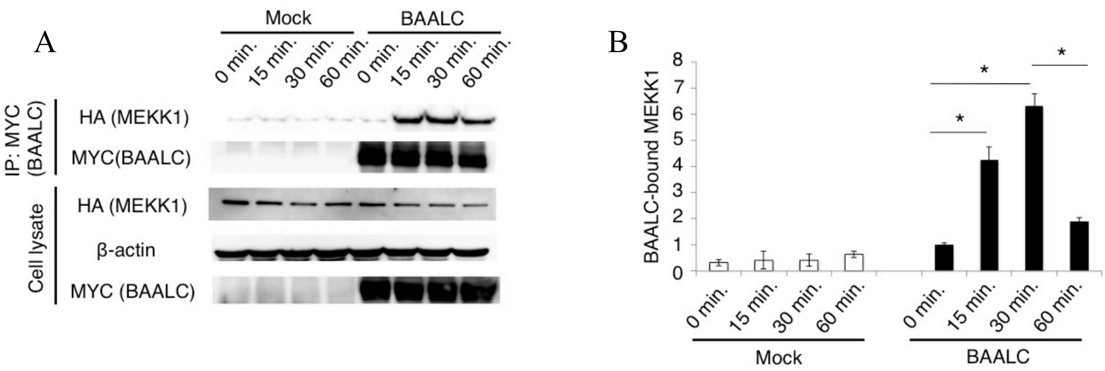


**Figure 17. BAALC interacts with MEKK1 stimulation dependently.**

(A) Interaction between BAALC and MEKK1. HEK293T cells were cotransfected with HA-tagged MEKK1 and MYC-tagged BAALC or MYC-tagged control vector. Cells were stimulated with EGF (10 ng/mL) for the indicated time periods. Immune complexes were precipitated by anti MYC-tag antibody and blotted by anti HA-tag antibody. (A) Representative immunoblot showing BAALC-bound MEKK1. (B) Cumulative data of the amount of MEKK1 bound to BAALC as represented in (E). Values were normalized to that of BAALC overexpressing HEL cells at 0 minute after EGF stimulation (n = 3)

Data are mean ± SEM values. * $P < 0.05$.

As for the interaction between ERK and MKP3, EGF treatment rapidly induced dissociation of MKP3 from ERK, followed by MKP3 reassociation with ERK after 30 minutes of stimulation in control cells. On the contrary, in BAALC-overexpressing cells, the recruitment of MKP3 to ERK at 30 minutes was hindered along with the stimulation-dependent BAALC-MEKK1 interaction up to 60 minutes after stimulation (Figure 18A and 18B).

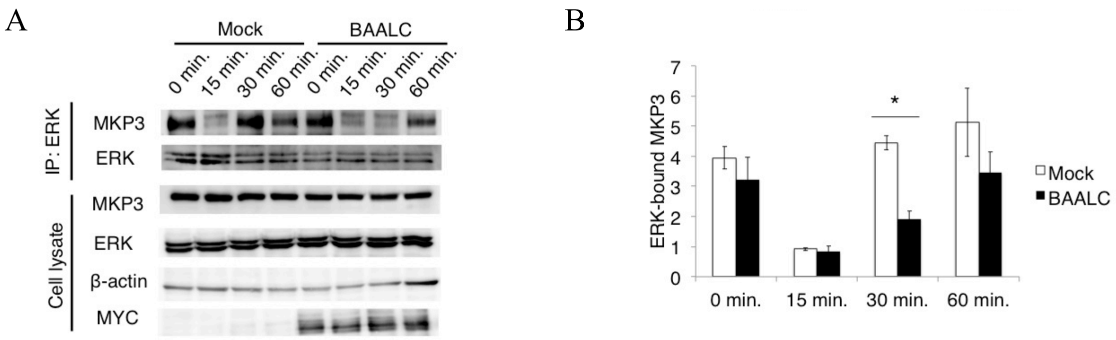


**Figure 18. BAALC blocks reassociation of MKP3 and ERK.**
(A) Interaction between ERK and MKP3. HEK293T cells were cotransfected with FLAG-tagged MKP3 and MYC-tagged BAALC or MYC-tagged control vector. Cells were stimulated with EGF (10 ng/mL) for the indicated time periods. Immune complexes were precipitated by anti-ERK antibody and ERK-bound MKP3 was detected by anti FLAG-tag antibody. (B) Cumulative data of the amount of MKP3 bound to ERK as represented in (A). Values were normalized to that of mock-transduced HEK293T cells taken at 15 minutes after EGF stimulation (n = 3). Data are mean ± SEM values. * $P < 0.05$.

The extent of ERK phosphorylation was inversely correlated to the intensity of the ERK-MKP3 interaction, underscoring the importance of MKP3 in determining ERK activity (Figure 19A and 19B).

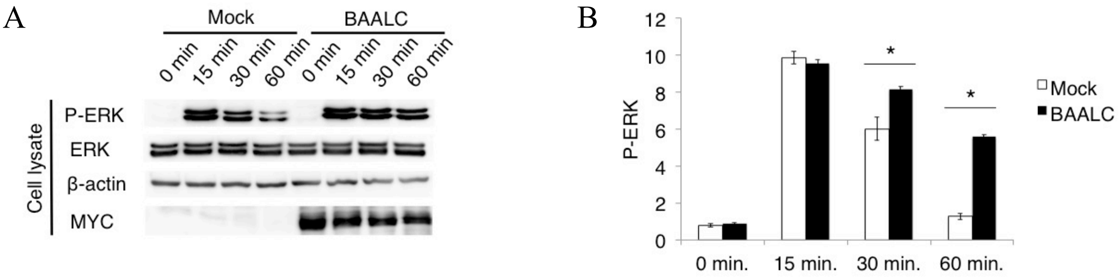


**Figure 19. Phosphorylation of ERK is positively regulated by the interaction of BAALC and MEKK1.**

Time lapse analysis of ERK activation in HEK293T cells transfected with BAALC or control vector. Cells were stimulated with 10 ng/mL EGF for the indicated time periods. (A) Immunobloting of phosphorylated ERK. (B) Cumulative data of the amount of phosphorylated ERK. Values are normalized to control sample taken at 0 minute after stimulation (n = 3).
Data are mean ± SEM values. * $P < 0.05$.

To verify that BAALC promotes proliferation of leukemia cells by inhibiting the function of MKP3, we evaluated the effect of MKP3 overexpression on BAALC-induced cell proliferation in HEL cells. U0126, a potent and specific inhibitor of MEK[41], inhibited proliferation in both control and BAALC-expressing HEL cells to a comparable level, completely abrogating the growth advantage conferred by BAALC (Figure 20).

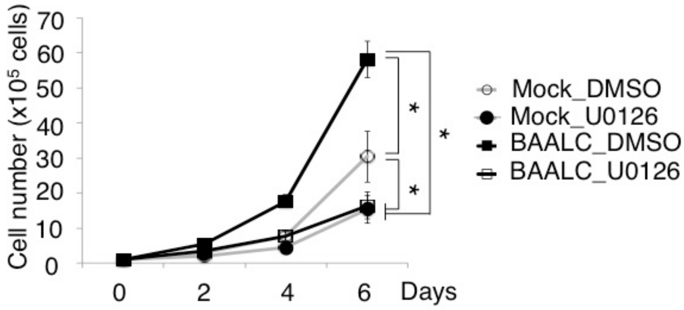


**Figure 20. Proliferative advantage of BAALC is canceled by MEK inhibition.**
Growth curve of HEL cells transduced with BAALC or control vector followed by treatment with U0126 (5 μM) or DMSO (n =3). Data are mean ± SEM values. * P < 0.05.

In addition, growth advantage of BAALC-expressing cells was reversed by forced expression of MKP3 (Figure 21A – 21C), suggesting that BAALC affects proliferative capacity of AML cells in a ERK-dependent manner.

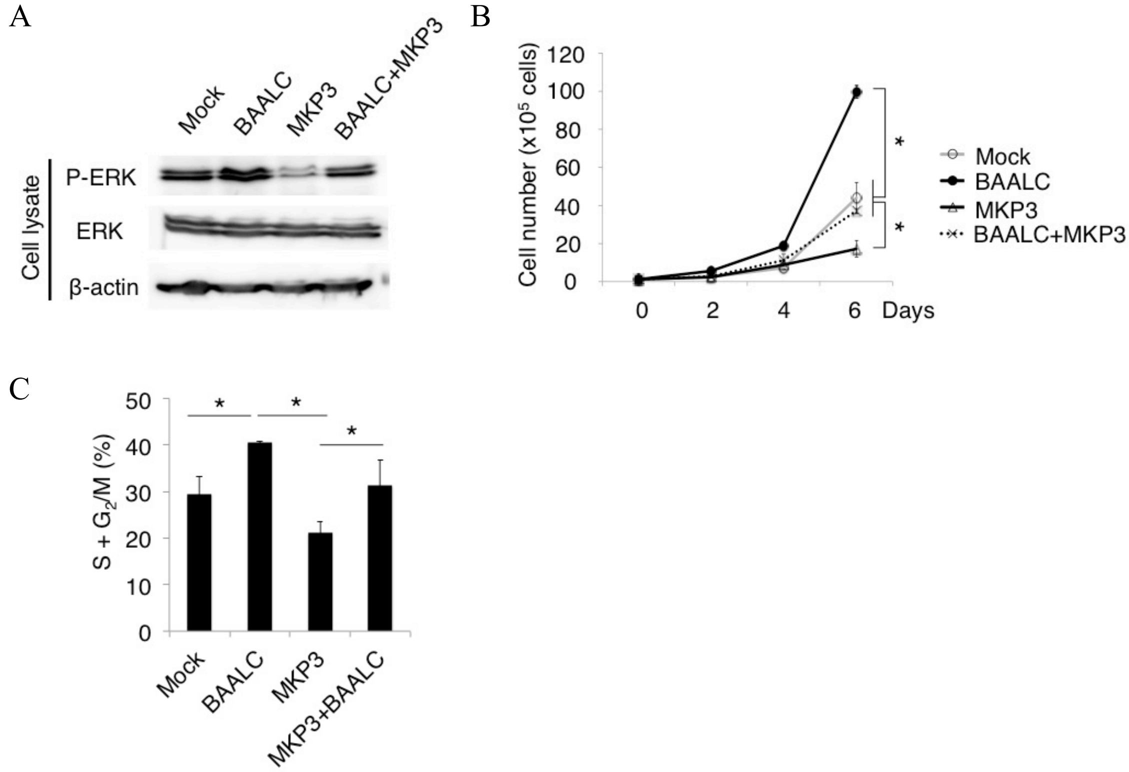

**Figure 21. BAALC and MKP3 competitively interact with ERK.**

(A) Immunobloting of phosphorylated ERK in HEL cells cotransduced with BAALC and MKP3. (B) Growth curve of HEL cells cotransduced with BAALC and MKP3 (n =3). (C) Cell cycle analysis (% of S and G2/M phase) of HEL cells cotransduced with BAALC and MKP3 (n =3). Data are mean ± SEM values. * P < 0.05.

These results collectively suggest that BAALC interacts directly with MEKK1, an essential scaffold protein for ERK activation, and induces prolonged ERK activation by inhibiting reassociation of MKP3 to ERK (Figure 22).

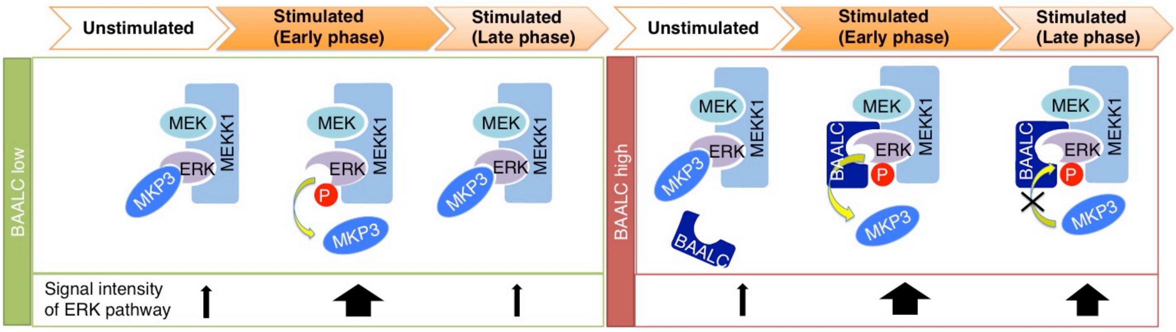


**Figure 22. BAALC works as an adaptor protein in ERK pathway.**

Schematic representation of the function of BAALC in ERK pathway. Molecular dynamics around MEKK1 were depicted. Time after ERK pathway activation was classified into three phases, un-stimulated phase (before EGF stimulation), early phase (0 to 30 minutes after EGF stimulation) and late phase (60 minutes after EGF stimulation and thereafter).

**BAALC induces drug resistance in AML cells through ERK activation.**

High BAALC expression is clinically associated with overexpression of genes involved in drug resistance, lower complete remission rate and refractoriness to chemotherapy in AML cases[11, 42]. Given that ERK can exert its oncogenic activity through increasing resistance to chemotherapeutic drugs[43, 44], we deduced that BAALC may lead to drug resistance via ERK pathway. ATP-binding cassette (ABC) proteins transport various molecules including incorporated cytotoxic agents across extra-and intra-cellular membranes and represent a major mechanism of drug resistance[45]. Among the superfamily of ABC transporters, ABCB1 (MDR1; multidrug resistance protein 1), ABCC1-5 (MRP1-5; multidrug resistance-associated protein-1-5) and ABCG2 (BCRP1; breast cancer resistance protein 1) are well-known downstream targets of ERK pathway[46-48]. To elucidate the role of BAALC-induced ERK activation in induction of drug resistance genes in BAALC-expressing cells, we treated AML cells with cytosine arabinoside (AraC), an essential component of AML treatment, and measured the mRNA expression of these ABC transporters. We found that additive BAALC expression in HEL cells potentiated the up-regulation of *ABCB1*, *ABCC1*, *ABCC4* and *ABCG2* in response to AraC treatment (Figure 23).

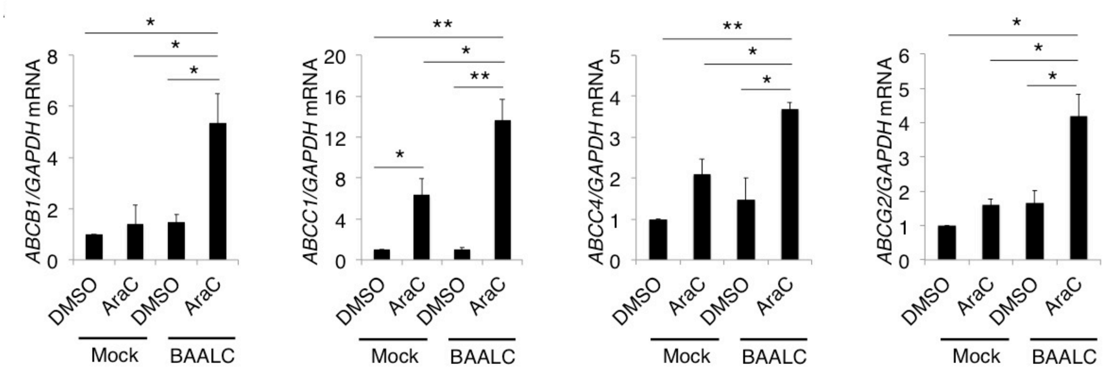


**Figure 23. BAALC induces expression of ABC transporter genes.**
Expression levels of ABC transporters (ABCB1, ABCC1, ABCC4 and ABCG2) in HEL cells transduced with BAALC or control vector followed by treatment with AraC (1 μM) or DMSO for 48 hours. Values were normalized to that of mock-transduced HEL cells treated with DMSO (n = 3). Data are mean ± SEM values. * $P < 0.05$, ** $P < 0.01$.

When the half-maximal inhibitory concentrations (IC50) were assessed, in line with the high expression of resistance-related genes, BAALC-expressing cells were more resistant to AraC treatment (Figure 24).

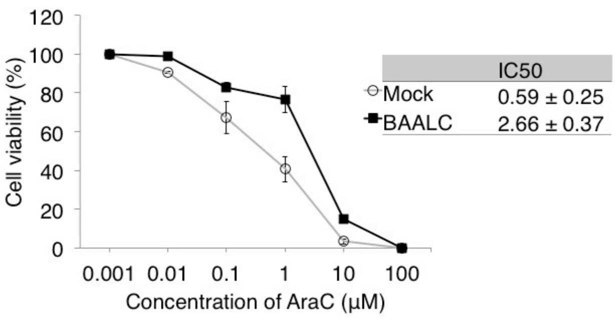

**Figure 24. BAALC induces resistance to AraC treatment in HEL cells.**

AraC sensitivity of HEL cells transduced with BAALC or control vector. Cells were treated with AraC at the indicated concentrations and cell viabilities were determined by trypan blue exclusion assays (n = 3). IC50 values of BAALC or mock overexpressing HEL cells are provided. Data are mean ± SEM values.

Up-regulation of these ABC transporters were abrogated in the presence of MEK inhibitor (Figure 25), indicating that BAALC-induced drug resistance is a MEK/ERK-dependent process.

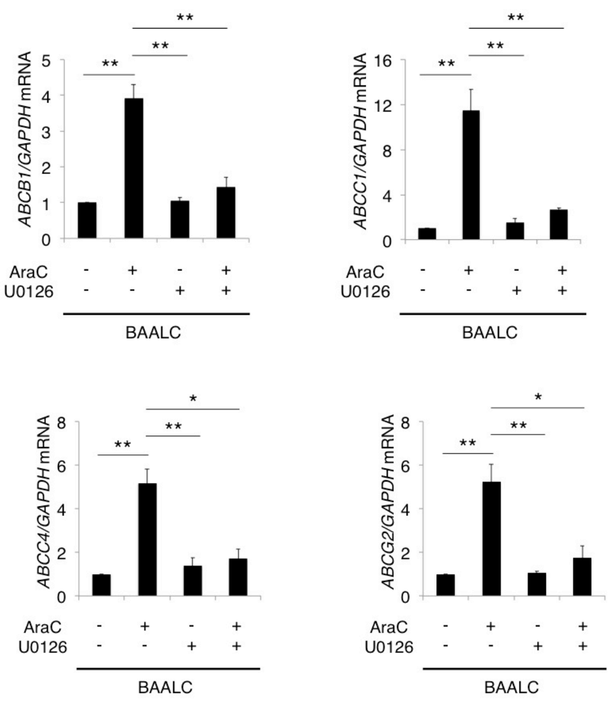


**Figure 25. BAALC-induced expression of ABC transporter genes is reverted by MEK inhibition.**

Expression levels of ABC transporters (ABCB1, ABCC1, ABCC4 and ABCG2) in HEL cells transduced with lentiviruses encoding BAALC followed by treatment with AraC (1 μM) or DMSO for 48 hours in the presence of U0126 (5 μM). Data was normalized to the result of BAALC transduced HEL cells with DMSO treatment (n = 3).

Data are mean ± SEM values. * $P < 0.05$, ** $P < 0.01$.

Consequently, MEK inhibitor overcame the chemoresistance of BAALC-expressing cells to AraC (Figure 26).

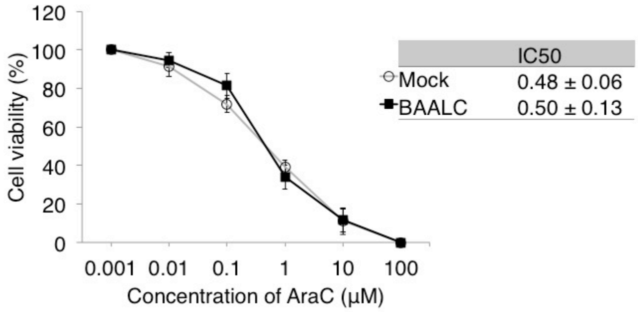


**Figure 26. MEK inhibition cancels BAALC-induced drug resistance in HEL cells.**
AraC sensitivity of HEL cells transduced with BAALC or control vector in the presence of U0126 (5 μM). Cells were treated with AraC at the indicated concentrations and cell viabilities were determined by trypan blue exclusion assays (n = 3). IC50 values of BAALC or mock overexpressing HEL cells are provided. Data are mean ± SEM values.

These results support the idea that BAALC induces drug resistance by up-regulating the expression of drug resistance genes in an ERK-dependent way, which also can be targeted by MEK inhibitor.

**Monocytic differentiation induced by constitutive activation of the ERK pathway is dependent on nuclear expression of KLF4.**

To address whether the growth-promoting effect of BAALC overexpression on leukemia cells was dependent on the ERK pathway, the constitutive active form of MEK1 (CA-MEK1, S218E/S222E) was transduced into HEL cells. In clear contrast to the case of BAALC overexpression, CA-MEK1 decreased cell proliferation (Figure 27A) and induced monocytic differentiation (Figure 27B and 27C), despite comparable phosphorylation of ERK (Figure 27D).

A

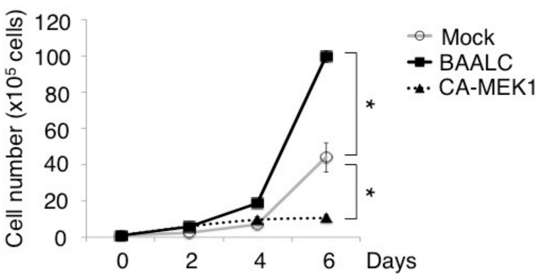


B

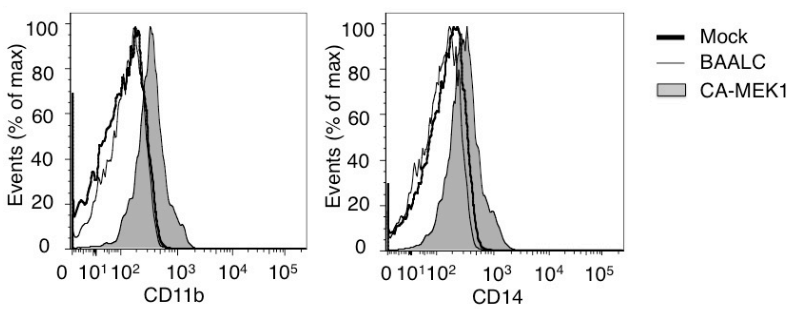

C

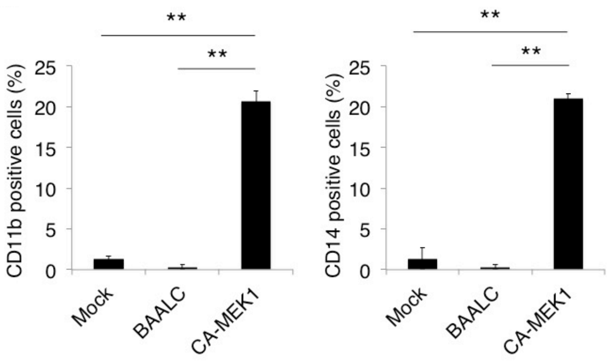


D

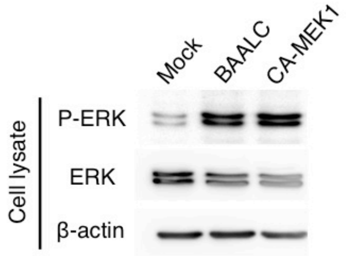


**Figure 27. Phenotypic discrepancy between BAALC and CA-MEK1.**

(A) Growth curve of HEL cells transduced with BAALC, CA-MEK1 or control vector (n = 3). (B) Representative flow cytometric data showing CD11b and CD14 expressions in Kasumi-1 cells transduced with BAALC, CA-MEK1 or control vector. (C) Cumulative data of the percentage of CD11b and CD14 positive cells (n = 3). (D) Immunoblotting of phosphorylated ERK in HEL cells transduced with BAALC, CA-MEK1 or control vector. Cells were stimulated by PMA (100 ng/mL) for 6 hours.

Data are mean ± SEM values. * $P < 0.05$, ** $P < 0.01$.

To further investigate this phenotypic discrepancy, we focused on a biological function of KLF4, another interacting partner of BAALC, the expression of which is positively regulated by ERK in tumor cells from several origins[25, 49]. Taken into account the involvement of KLF4 in monocytic differentiation of myeloid cells[27, 50], it was supposed that KLF4 may have some role in ERK-independent action of BAALC. Given KLF4 exerts transcription activating potential in the nucleus as a transcription factor with zinc-finger motifs[38], the amount of KLF4 in the nucleus is considered to be of importance. When we compared the expression levels of KLF4 by immunoblotting, nuclear expression of KLF4 was increased in CA-MEK1-transduced HEL cells, accompanied by increase of KLF4 in whole cell lysates (Figure 28).

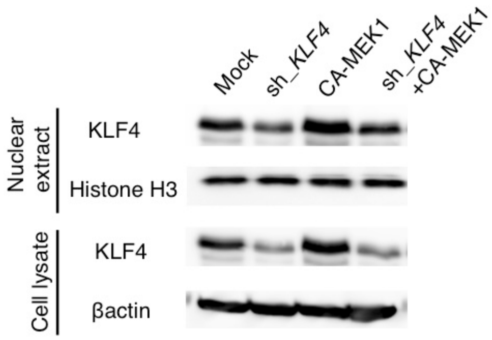


**Figure 28. Constitutive activation of ERK pathway induces KLF4 accumulation in the nucleus.**

Immunoblotting of total and nuclear KLF4 in HEL cells cotransduced with KLF4 (sh_KLF4) and CA-MEK1.

When KLF4 was knocked down by shRNA in this context, CA-MEK1-induced growth arrest was reversed along with decreased KLF4 expression in the nucleus, although knockdown of KLF4 had little effect on the proliferative capacity in the absence of constitutive activation of ERK (Figure 29).

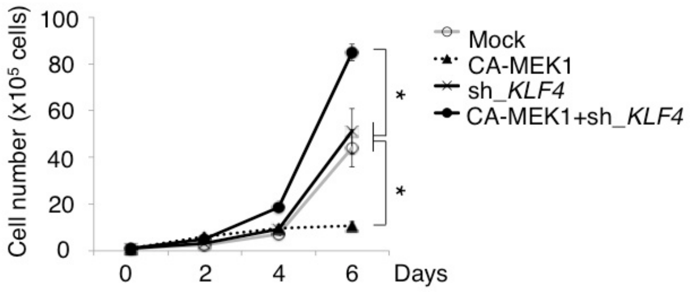


**Figure 29. Growth suppression of CA-MEK1 is canceled by KLF4 knockdown in HEL cells.**

Growth curve of HEL cells cotransduced with sh_KLF4 and CA-MEK1 (n = 3).

Data are mean ± SEM values. * $P < 0.05$.

CA-MEK1-induced differentiation was also counteracted by KLF4 depletion assessed by flow cytometric analyses of monocyte differentiation markers (Figure 30A and 30B).

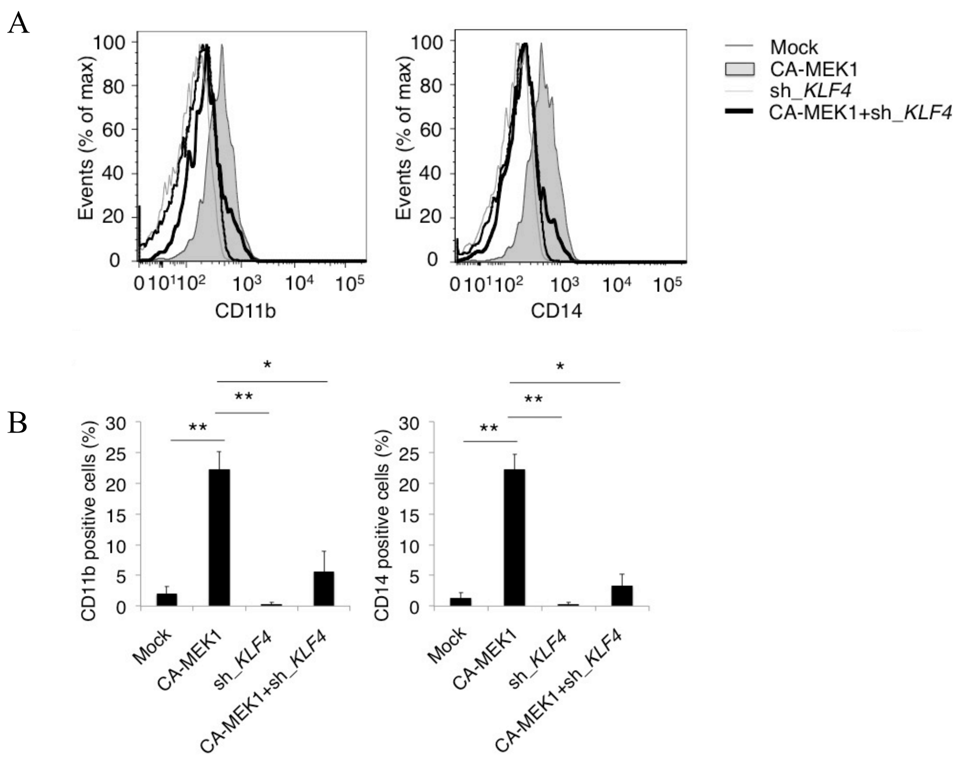

**Figure 30. CA-MEK1-induced monocytic differentiation of HEL cells is canceled by KLF4 knockdown.**

(A) Representative flow cytometric data showing CD11b and CD14 expressions in HEL cells cotransduced with sh_KLF4 and CA-MEK1. (B) Cumulative data of the frequency of CD11b and CD14 positive cells (n =3). Data are mean ± SEM values.* P < 0.05, ** P < 0.01.

KLF4 knockdown also inhibited up-regulation of monocytic differentiation-related genes (*CES1, CSF1R, MAFB*) induced by CA-MEK1 (Figure 31).

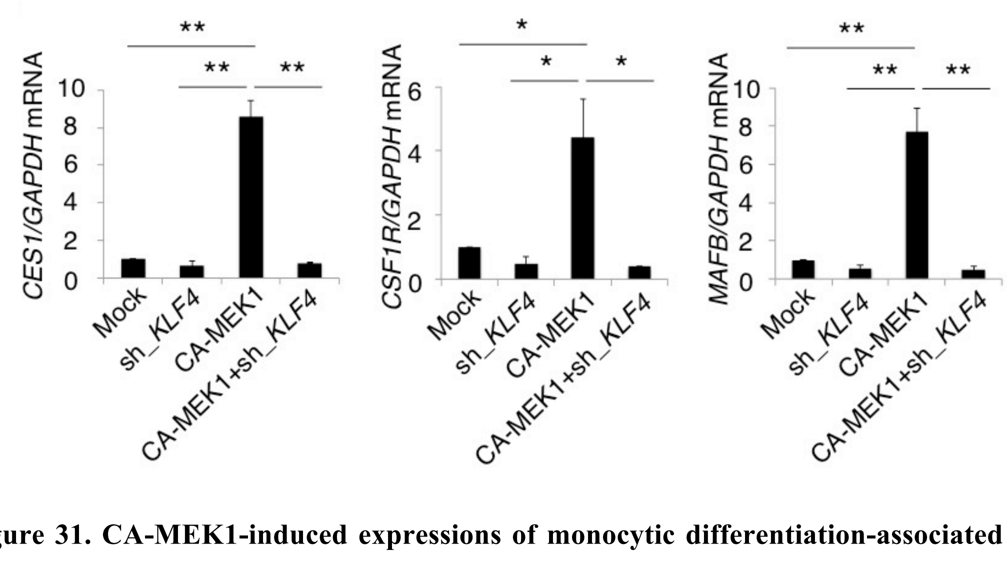


**Figure 31. CA-MEK1-induced expressions of monocytic differentiation-associated genes are reverted by KLF4 knockdown.**

Expressions of monocytic differentiation-associated genes (CES, CSF1R and MAFB) in HEL cells cotransduced with sh_KLF4 and CA-MEK1 (n = 3). Values were normalized to that of mock-transduced HEL cells.

Data are mean ± SEM values.* P < 0.05, ** P < 0.01.

Morphologic analysis revealed that CA-MEK1-expressing cells exhibited marked changes characterized by increased cell volume, typical folded nuclei with decreased nuclear/cytoplasmic ratio and vacuoles in the cytoplasm, consistent with monocytic phenotype. Simultaneous expression of KLF4 shRNA reversed CA-MEK1-induced morphological change (Figure 32).

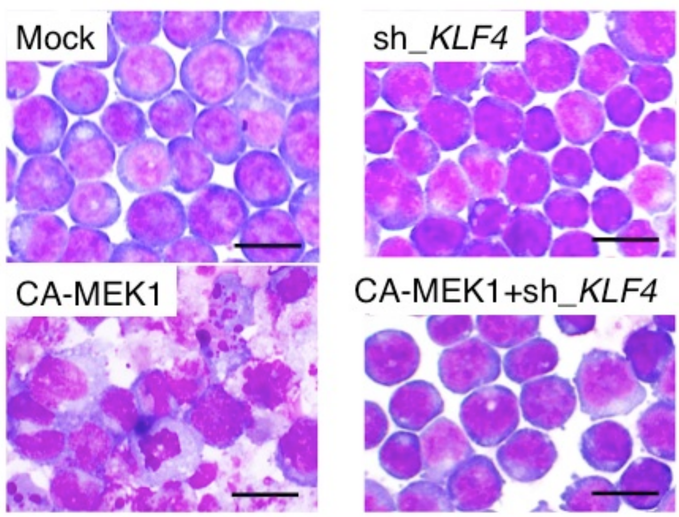


**Figure 32. CA-MEK1-induced monocytic change is reverted by KLF4 knockdown.**
Representative images of May-Giemsa stained HEL cells cotransduced with sh_KLF4 and CA-MEK1 (scale bars, 50 μm).

These data indicates that sustained activation of ERK pathway induces monocytic differentiation in leukemia cells in a KLF4-dependent manner.

**BAALC antagonizes increased KLF4 activity through ERK activation and inhibition of nuclear KLF4 localization.**

Since BAALC- and CA-MEK1-overexpressing cells commonly showed prolonged ERK activation, we further investigated the difference between BAALC and CA-MEK1 in cell proliferation. When BAALC was transfected into HEK293T cells, immunofluorescence microscopy revealed that KLF4 translocated from nucleus to cytoplasm (Figure 33).

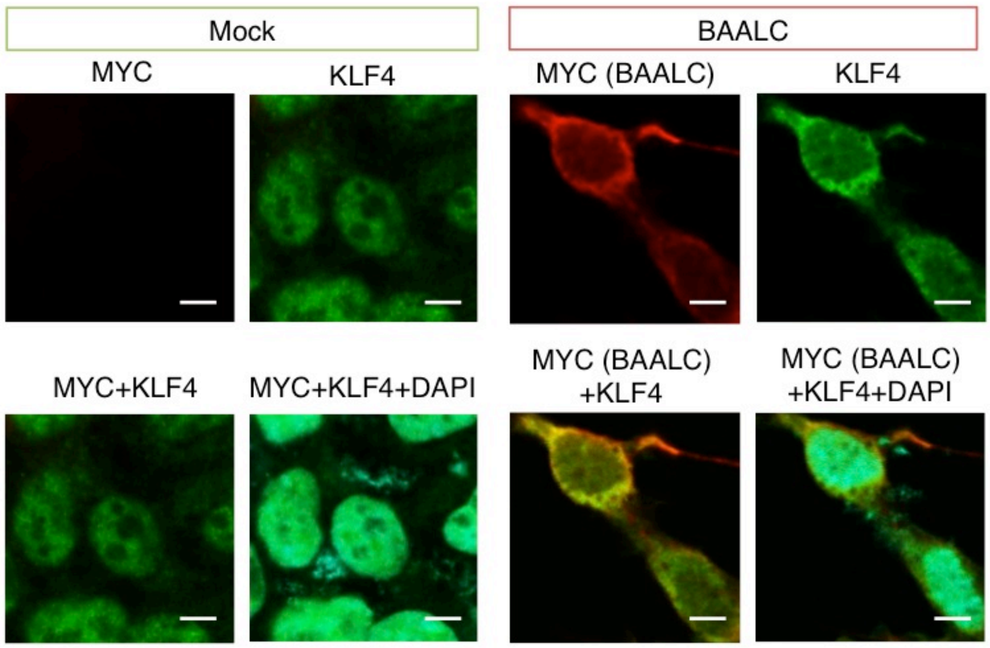


**Figure 33. BAALC overexpression drives translocation of KLF4 from the nucleus to the cytoplasm.**
Immunofluorescence images of KLF4 in HEK293T cells transduced with MYC-tagged BAALC or control vector (scale bars, 10 μm).

On the contrary, knocking-down of BAALC in Kasumi-1 cells, had cytoplasmic KLF4 shift to nucleus (Figure 34).

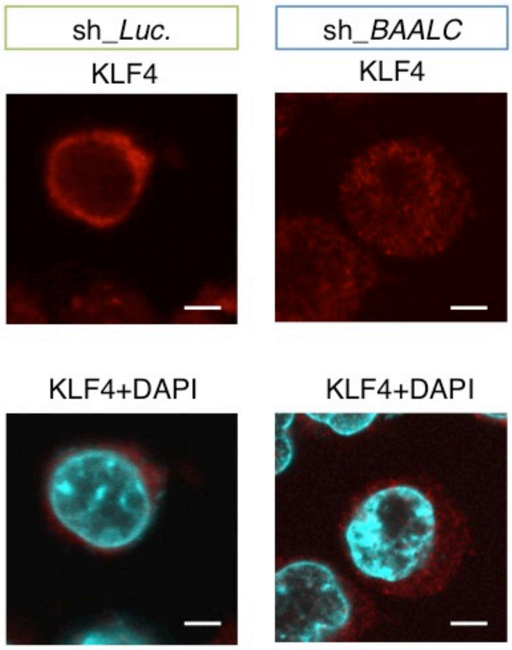


**Figure 34. Knockdown of BAALC induces translocation of KLF4 from the cytoplasm to the nucleus.**

Immunofluorescence images of KLF4 in Kasumi-1 cells transduced with sh_Luc. or sh_BAALC (scale bars, 10 μm).

Immunoblotting of nuclear extracts from these cells showed that the amount of KLF4 in the nucleus was decreased by BAALC overexpression and increased by BAALC-knockdown, and the amount of cytoplasmic KLF4 inversely related to that of nuclear KLF4 (Figure 35A – 35D).

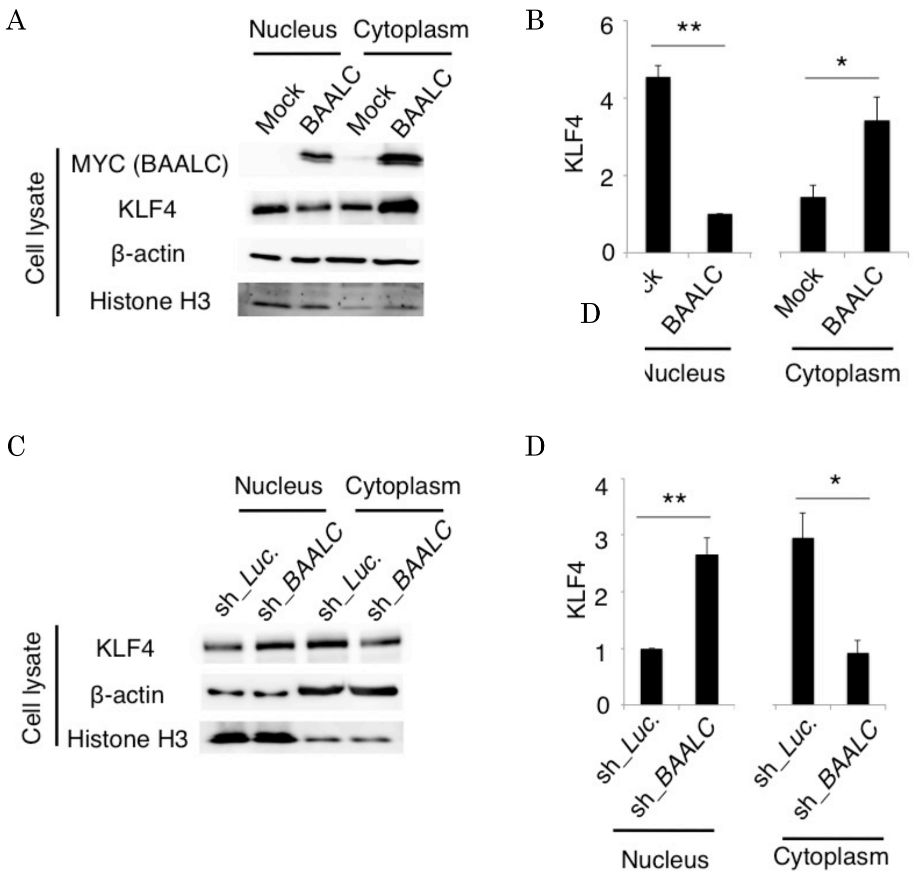


**Figure 35. BAALC holds KLF4 in the cytoplasm and blocks its nuclear translocation.**
(A) Immunoblotting of KLF4 in the nuclear and cytoplasmic fractions of HEK293T cells transduced with MYC-tagged BAALC or control vector. (B) Cumulative data of the amount of KLF4 as represented in (A). Values were normalized to that of nuclear fraction from BAALC overexpressing HEK293T cells (n = 3). (C) Immunoblotting of KLF4 in the nuclear and cytoplasmic fractions of Kasumi-1 cells transduced with sh_Luc. or sh_BAALC. (D) Cumulative data of the amount of KLF4 as represented in (C). Values were normalized to that of nuclear fraction from control vector transduced Kasumi-1 cells (n = 3).
Data are mean ± SEM values. * $P < 0.05$, ** $P < 0.01$.

When $CD34^+$ $CD38^-$ bone marrow cells from AML patients were assessed for KLF4 localization, BAALC-high cases (the upper quartile of *BAALC* expression) mainly showed cytoplasmic KLF4, while KLF4 was proportionally distributed both in the nucleus and the cytoplasm in BAALC-low cases (the lower quartile) (Figure 36A and Figure 36B).

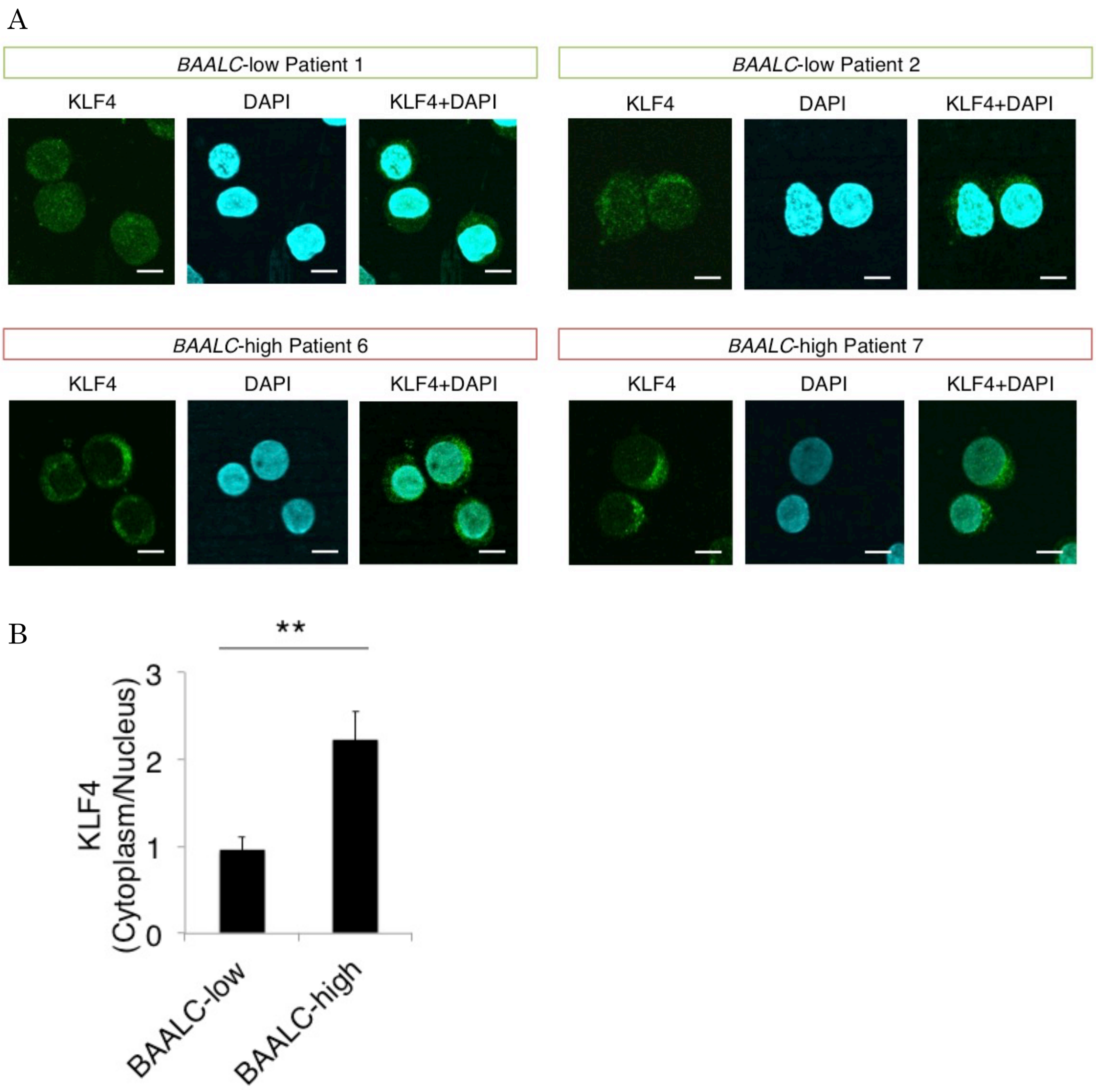


**Figure 36. BAALC blocks nuclear translocation of KLF4 in human AML bone marrow cells.**

(A) Immunofluorescence images of KLF4 in $CD34^{+}$ $CD38^{-}$ bone marrow cells from AML patients. Representative images from two AML patients with high and low BAALC expression were shown (scale bars, 10 μm). (B) Cumulative data of cytoplasm-nucleus ratio of KLF4 in CD34+ CD38- bone marrow cells from five AML patients with high and low BAALC expression respectively. Data are mean ± SEM values. ** P < 0.01.

To prove the hypothesis that BAALC inhibits ERK-mediated monocytic differentiation by relocating KLF4 from the nucleus to the cytoplasm, we examined whether the growth arrest with monocytic differentiation in CA-MEK1-expressing HEL cells could be overcome by additional BAALC expression. Indeed, BAALC overexpression in CA-MEK1-transduced HEL cells restored proliferative capacity (Figure 37).

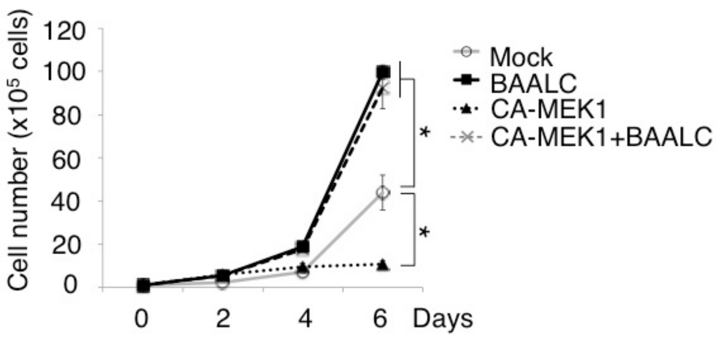


**Figure 37. CA-MEK1-induced growth suppression of HEL cells is reverted by additional BAALC expression.**

Growth curve of HEL cells cotransduced with BAALC and CA-MEK1 (n = 3).

Data are mean ± SEM values. * P < 0.05.

CA-MEK1-expressing cells with simultaneous BAALC expression were resistant to CA-MEK1-induced differentiation, determined by flow cytometric quantification of CD11b and CD14 (Figure 38A and 38B).

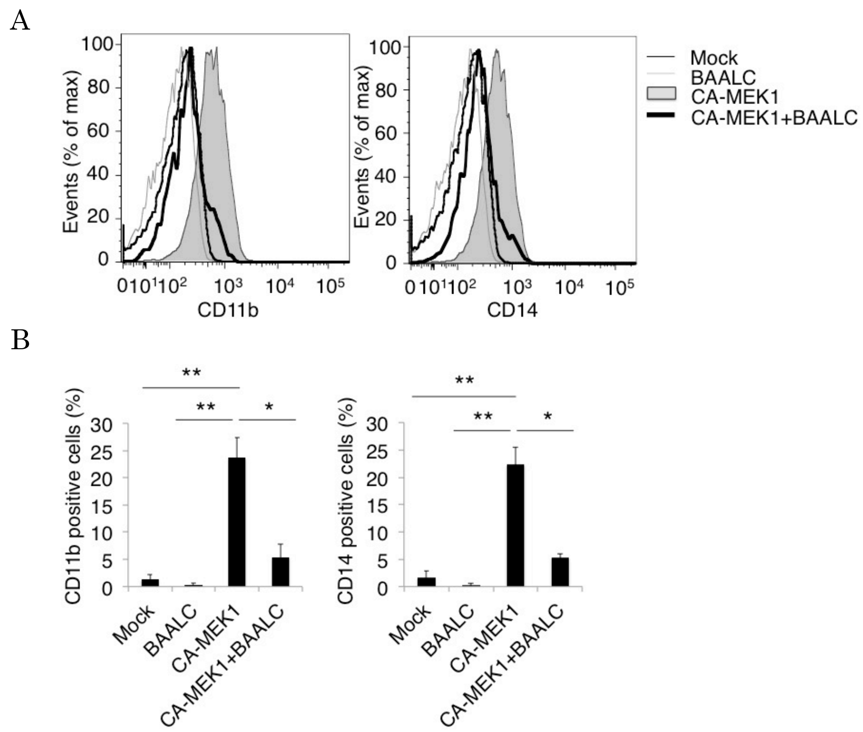


**Figure 38. CA-MEK1-induced monocytic differentiation in HEL cells is reverted by additional BAALC expression.**

(A and B) Monocytic differentiation assessed by expressions of CD11b or CD14 in HEL cells cotransduced with BAALC and CA-MEK1. (A) Representative flow cytometric data. (B) Cumulative data from three independent experiments.

Data are mean ± SEM values. * $P < 0.05$, ** $P < 0.01$.

BAALC blocked induction of differentiation-associated genes in CA-MEK1-expressing cells (Figure 39).

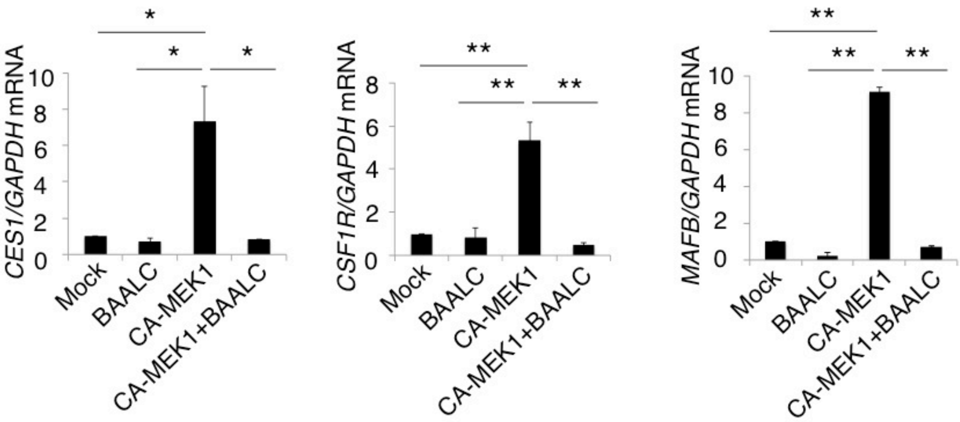


**Figure 39. CA-MEK1-induced expression of monocytic differentiation-associated genes in HEL cells is reverted by additional BAALC expression.**

Expression levels of monocytic differentiation-associated genes (CES, CSF1R and MAFB) in HEL cells cotransduced with BAALC and CA-MEK1. Values are normalized to the expression levels in control vector-transduced HEL cells (n = 3).

Data are mean ± SEM values. * $P < 0.05$, ** $P < 0.01$.

Microscopic analysis also revealed that the morphological features of monocytes seen in CA-MEK1-transduced cells were abrogated by concomitant BAALC expression (Figure 40).

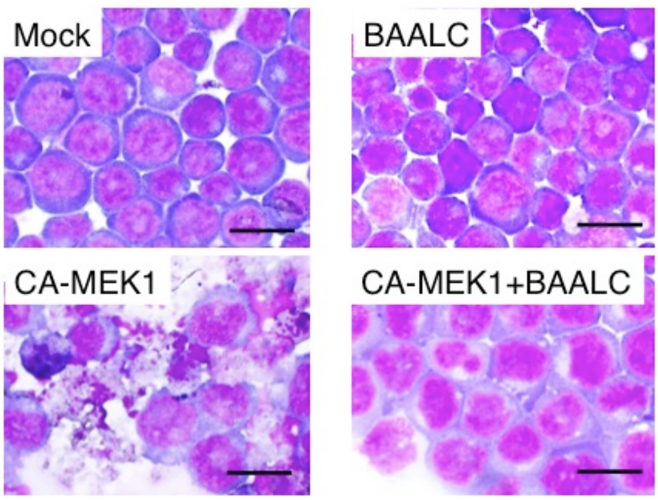

**Figure 40. CA-MEK1-induced monocytic change in HEL cells is reverted by additional BAALC expression.**
Representative images of May-Giemsa stained HEL cells cotransduced with BAALC and CA-MEK1 (scale bars, 50 μm).

The amount of KLF4 in the nucleus was reduced by BAALC in CA-MEK1-expressing cells (Figure 41), supporting the hypothesis that BAALC blocks ERK-dependent differentiation by affecting the amount of KLF4 in the nucleus.

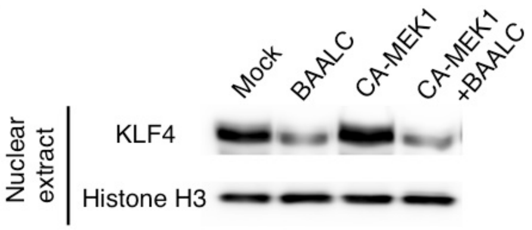


**Figure 41. CA-MEK1- induced accumulation of KLF4 in the nucleus is canceled by additional BAALC expression in HEL cells.**
Immunoblotting of KLF4 in the nuclear fractions of HEL cells cotransduced with BAALC and CA-MEK1.

To further elucidate the role of KLF4 in BAALC-derived proliferation and differentiation block with prolonged ERK activation, we assessed whether differentiation block in HEL cells by BAALC could be reversed by additional expression of KLF4. As expected, KLF4 overexpression restored nuclear KLF4

(Figure 42A) and decreased proliferation in BAALC-expressing HEL cells (Figure 42B).

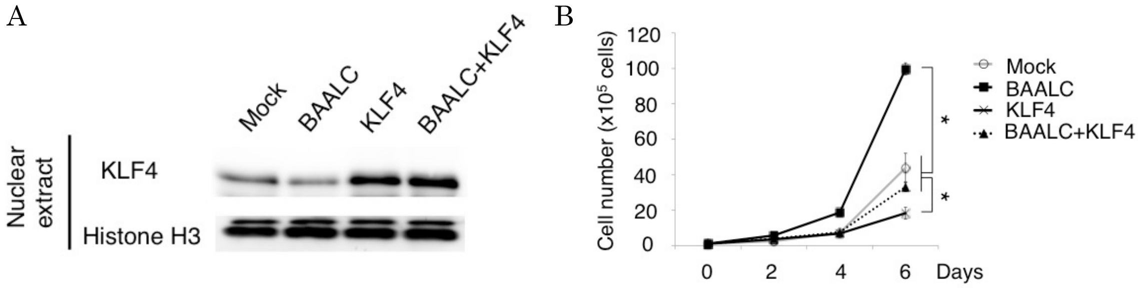


**Figure 42. BAALC-induced proliferative advantage in HEL cells is canceled by additional KLF4 expression.**

(A) Immunoblotting of nuclear KLF4 in HEL cells cotransduced with BAALC and KLF4. (B) Growth curve of HEL cells cotransduced with lentiviruses encoding BAALC or control Venus and lentiviruses enco Growth curve of HEL cells cotransduced with BAALC and KLF4 (n = 3).

Data are mean ± SEM values. * P < 0.05.

KLF4 induced monocytic differentiation regardless of BAALC expression, abrogating the differentiation block caused by BAALC (Figure 43A – 43D).

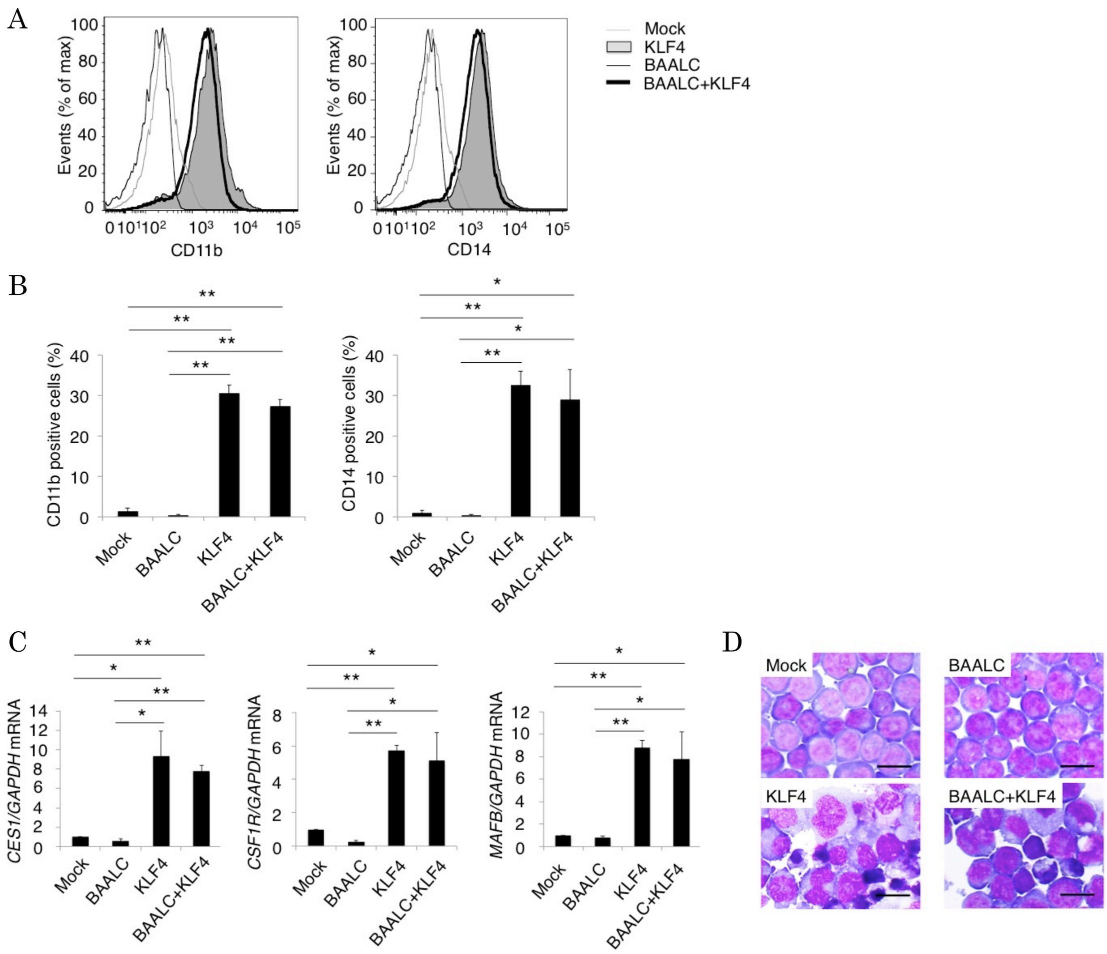


**Figure 43. Additional expression of KLF4 induces monocytic differentiation in BAALC-overexpressed HEL cells.**

(A and B) Monocytic differentiation assessed by expressions of CD11b or CD14 in HEL cells cotransduced with BAALC and KLF4. (A) Representative flow cytometric data. (B) Cumulative data from three independent experiments. (C) Expression levels of monocytic differentiation-associated genes (CES, CSF1R and MAFB) in HEL cells cotransduced with BAALC and KLF4. Values are normalized to the expression levels in control vector-transduced HEL cells (n = 3). (D) Representative images of May-Giemsa-stained HEL cells cotransduced with BAALC and KLF4. (scale bars, 50 μm).

Data are mean ± SEM values. * $P < 0.05$, ** $P < 0.01$.

Furthermore, the mRNA expression of key regulators of cell cycle progression positively regulated by ERK, such as cyclin dependent kinase 6 (*CDK6*) and cyclin D1 (*CCND1*)[51], were consistently increased in BAALC-expressing HEL cells and decreased in Kasumi-1 cells transduced with BAALC shRNA. Meanwhile, the expression of cyclin-dependent kinase inhibitor 1 (*CDKN1A*, *p21*), an essential factor for KLF4-mediated tumor suppression as a major transactivation target of KLF4[52] was consistently decreased in HEL cells with BAALC overexpression and increased in BAALC-knocked-down Kasumi-1 cells (Figure 44A and 44B). These findings collectively indicate that BAALC promotes cell cycle progression by activating ERK pathway, and inhibits monocytic differentiation by inhibiting the function of KLF4 via nucleo-cytoplasmic translocation.

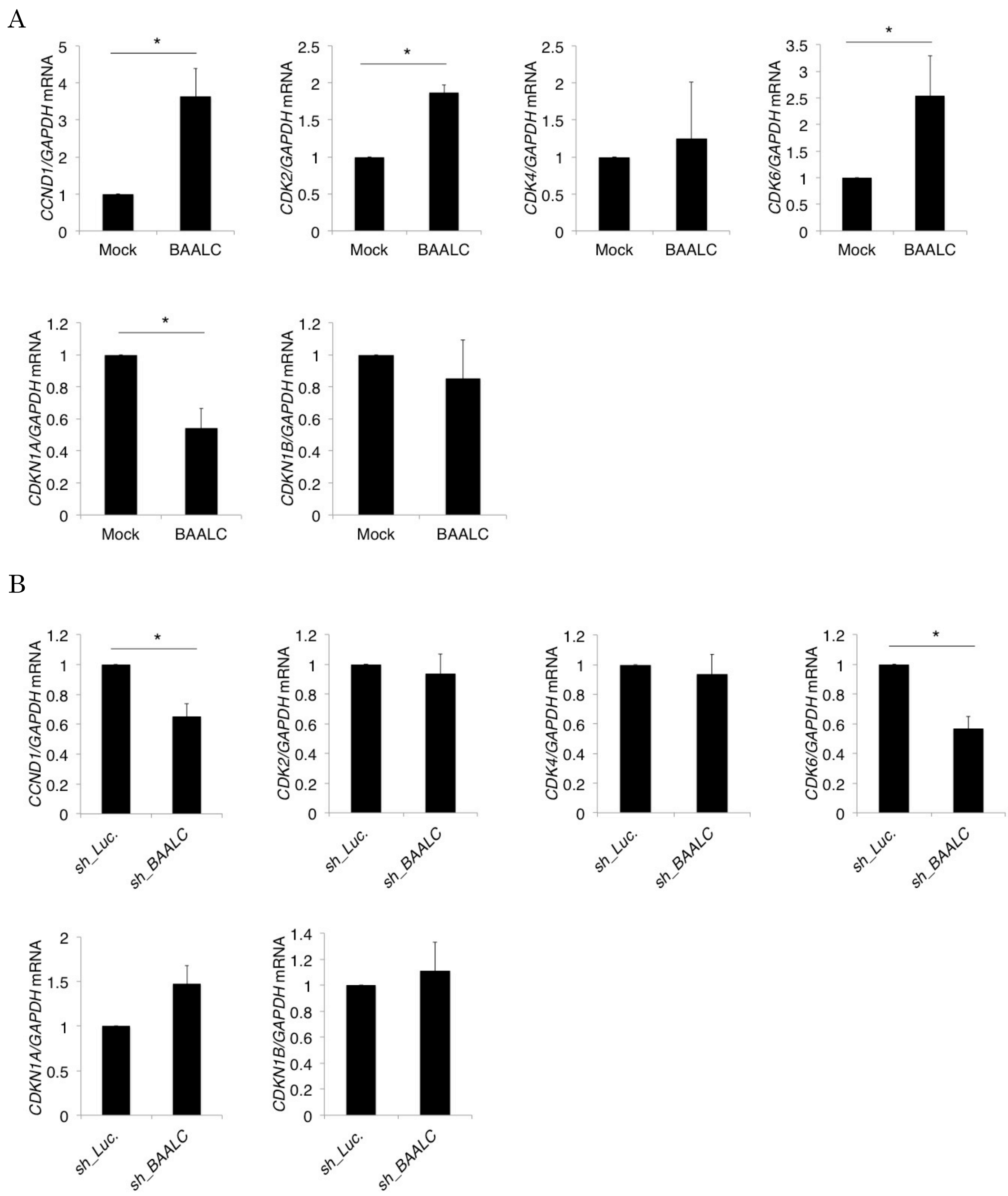


**Figure 44. BAALC modulates mRNA expressions of downstream targets of ERK and KLF4.**

(A) Expression levels of downstream target genes of ERK and KLF4 (CCND1, CDK2, CDK4, CDK6, CDKN1A and CDKN1B) in HEL cells transduced with BAALC or control vector. Values are normalized to the expression levels in control vector-transduced HEL cells (n = 3). (B) Expression levels of CCND1, CDK2, CDK4, CDK6, CDKN1A and CDKN1B in Kasumi-1 cells transduced with sh_Luc. or sh_BAALC #1. Values are normalized to the

expression levels in control vector-transduced Kasumi-1 cells (n = 3).
Data are mean ± SEM values. * $P < 0.05$.

**MEK/ERK inhibition in combination with KLF4 induction is a potential therapeutic strategy against BAALC-high AML.**

From the above-mentioned data, it is suggested that modulating ERK pathway and KLF4 expression would be an attractive target for treating BAALC-high leukemia. Thus we established tetracycline-inducible (Tet-ON) KLF4-expressing AML cell lines, in which KLF4 expression is induced by doxycycline. Although the effect of U0126 on differentiation of BAALC-expressing cells was marginal, KLF4 induction by doxycycline potently induced monocytic differentiation in these cells (Figure 45).

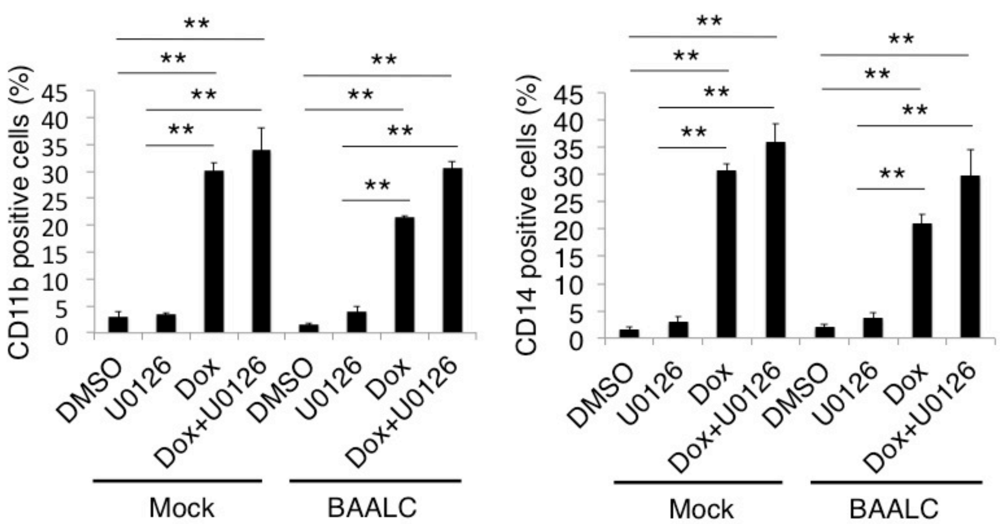

**Figure 45. Doxycycline-induced expression of KLF4 invoked monocytic differentiation in BAALC-overexpressed HEL cells.**

Cumulative data showing CD11b or CD14 expressions in HEL cells cotransduced with BAALC and Tet-ON KLF4 followed by treatment with U0126 (5 μM) or Dox (1 μM) or both. Data are mean ± SEM values. ** $P < 0.01$.

Given that BAALC exerts dual action on leukemia cells through ERK and KLF4, we evaluated the efficacy of combination therapy with MEK inhibition plus KLF4 induction in Kasumi-1 cells. Of note, there was an additional inhibitory effect of MEK inhibition and KLF4 induction on cell proliferation (Figure 46A), possibly reflecting accelerated differentiation induced by KLF4 (Figure 46B and 46C).

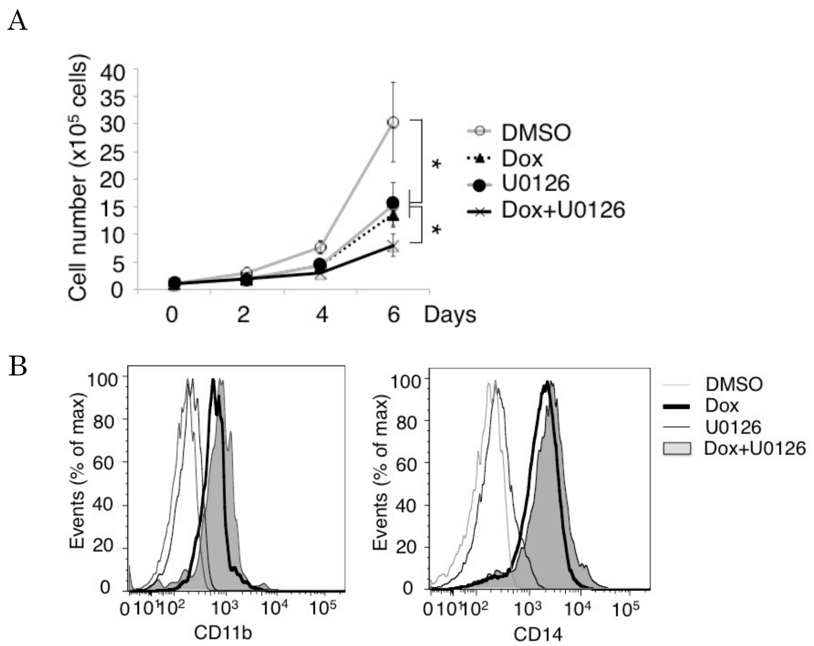

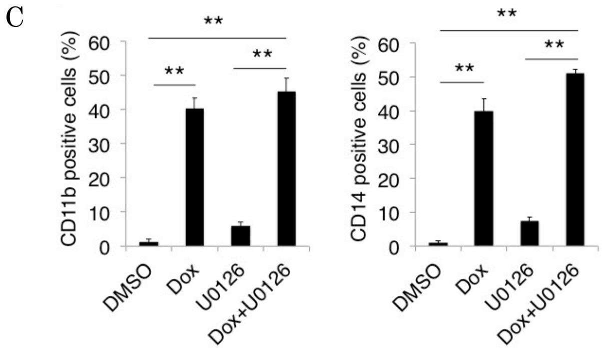


**Figure 46. MEK inhibition and KLF4 induction differentially affect Kasumi-1 cells.**
(A) Growth curve of Kasumi-1 cells transduced with tetracycline-inducible (Tet-ON) KLF4 treated with DMSO or U0126 (5 μM) combined with PBS or doxycycline (Dox; 1 μM) (n = 3).. (B and C) Monocytic differentiation assessed by expressions of CD11b or CD14 in Kasumi-1 cells transduced with Tet-ON KLF4 followed by treatment with U0126 (5 μM) or Dox (1 μM) or both. (B) Representative flow cytometric data. (C) Cumulative data from three independent experiments.
Data are mean ± SEM values. * P < 0.05, ** P < 0.01.

We next assessed the effect of MEK inhibition on the proliferation of several AML cell lines. Interestingly, sensitivity to MEK inhibitor was positively correlated to *BAALC* expression level (Figure 47).

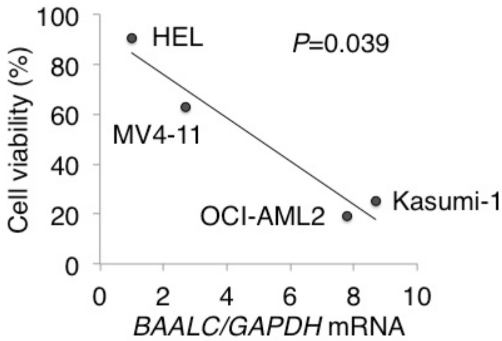


**Figure 47. Correlation between *BAALC* expressions and sensitivities to MEK inhibitor in AML cell lines.**

Expression of BAALC in AML cell lines and their sensitivity to U0126 was compared and Pearson's product-moment correlation coefficient was calculated.

The proliferation of AML cell lines with high BAALC (Kasumi-1, OCI-AML2) was effectively inhibited at 15-25 fold lower concentration of U0126 compared to cells with low BAALC (MV4-11, HEL) (Figure 48).

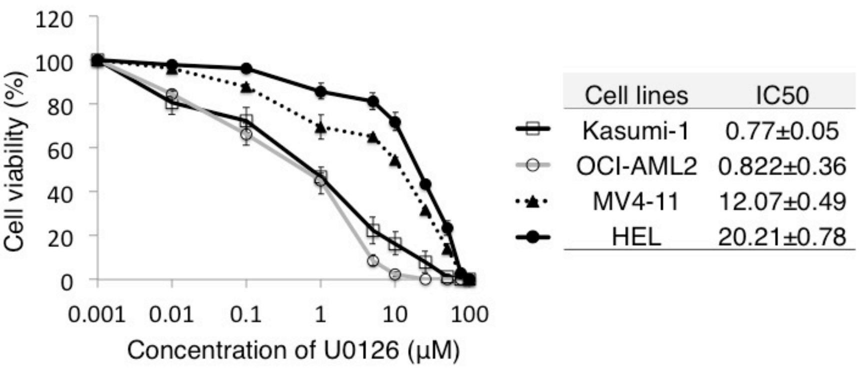


**Figure 48. Sensitivity to U0126 in AML cell lines.**

AML cell lines were treated with U0126 at the indicated concentrations and cell viabilities were determined by trypan blue exclusion assays (n = 4). IC50 value of each cell line is provided.

*BAALC* expression was also positively correlated to in vitro sensitivity to U0126 among primary human AML cells (Figure 49), highlighting MEK/ERK pathway as a legitimate therapeutic target in AML with high BAALC expression.

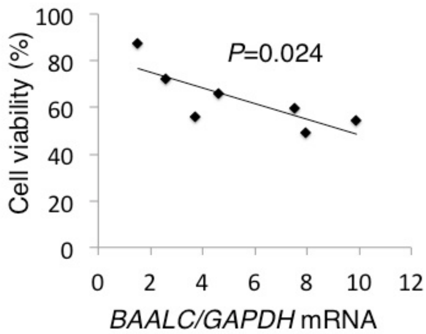


**Figure 49. Correlation between BAALC expressions and sensitivities to MEK inhibitor in human bone marrow cells from AML patients.**

Sensitivity to U0126 of CD34+CD38- fractions in bone marrow cells from AML patients (n = 7) and their *BAALC* expression was compared and Pearson's product-moment correlation coefficient was calculated.

Finally, we developed BAALC-high AML model mice using NOD/SCID/gamma (NSG) mouse to investigate the combinational effect of MEK inhibition and KLF4 induction in vivo (Figure 50).

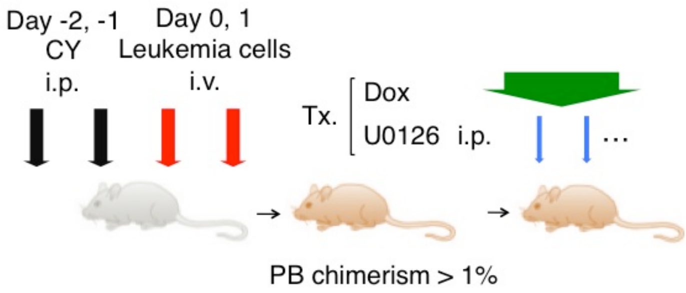


**Figure 50. Schematic design of xenograft mouse models of human AML.**

A xenograft mouse model of human AML with high expression of BAALC was developed using NSG mice. Before transplantation, NSG mouse was treated with i.p. injection of cyclophosphamide. At day 0 and day 1, Kasumi-1 cells were i.v. injected. Once PB chimerism of leukemia cells exceeded 1 %, treatment either by U0126 or doxycycline was started.

After intraperitoneal injection of cyclophosphamide for 2 days, Kasumi-1 cells expressing either BAALC shRNA or control shRNA were transplanted intravenously and the overall survival was evaluated. These xenotransplants succumbed to AML characterized by extensive infiltration of human $CD45^{+}$ leukemia cells in the BM, the liver and the spleen (Figure 51A and 51B).

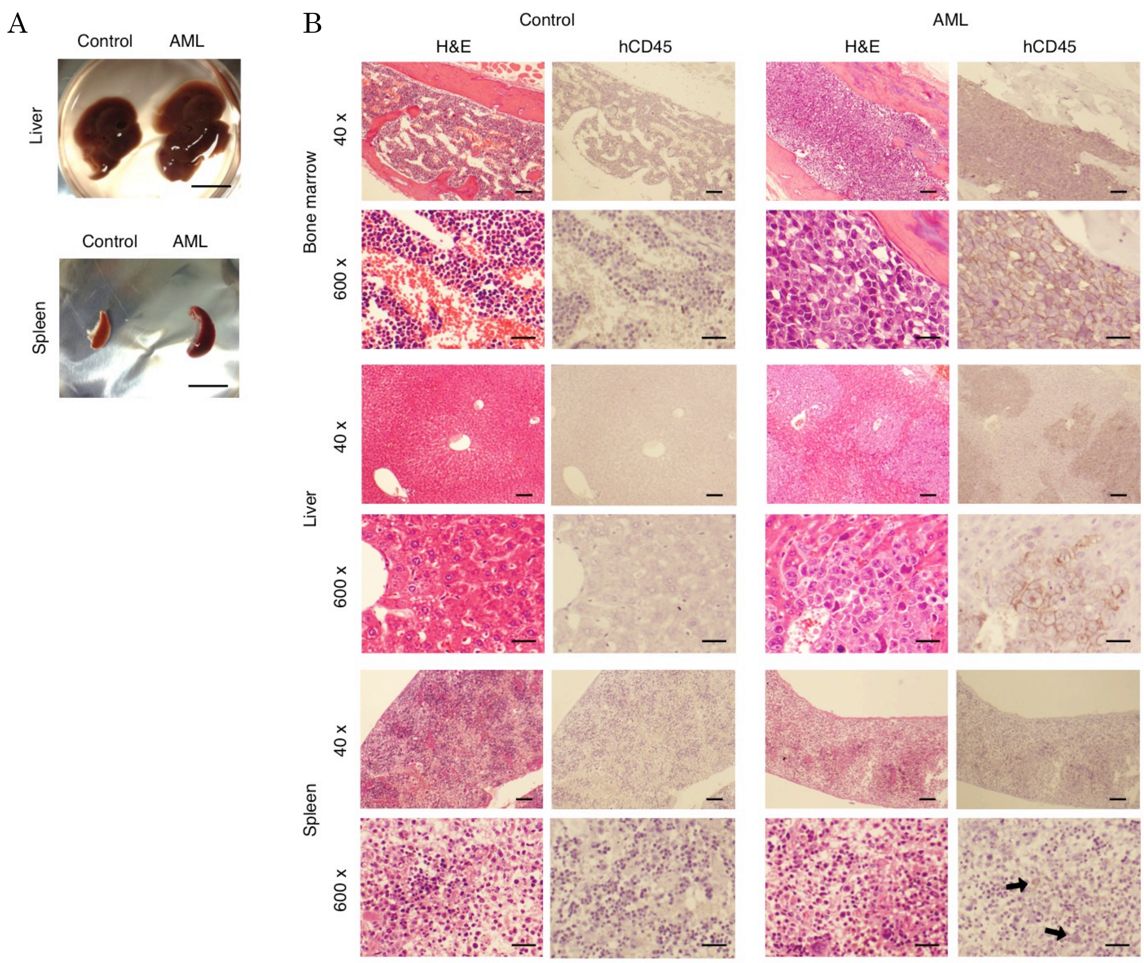


**Figure 51. Establishment of xenograft mouse model.**

(A) Representative macroscopic pictures of livers and spleens from a human AML xenograft mouse and a normal NSG control mouse (scale bars, 1cm). (B) Microscopic analyses of the bone marrow, the liver and the spleen from a human AML xenograft mouse and a normal NSG control mouse. Hematoxylin and eosin (H&E) staining and immunohistochemical staining with anti-human CD45 antibody were done for each slide (original magnification 40× and 600×, Scale bars, 200 μm in 40× and 20 μm in 600× images. Arrows in the spleen from a human AML xenograft mouse show hCD45+ cells.)

BAALC shRNA had a positive effect on mice transplanted with Kasumi-1 cells to prolong their survival, recapitulating the adverse prognostic impact of high BAALC expression in human AML (Figure 52).

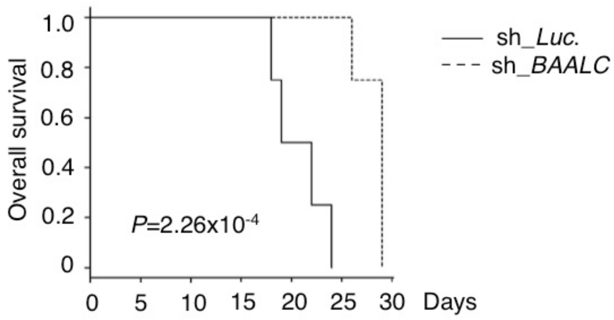


**Figure 52. NSG mice transplanted with Kasumi-1 cells recapitulate human AML with high expression of BAALC.**

Overall survival of NSG mice transplanted with Kasumi-1 cells transduced with sh_*Luc.* or sh_*BAALC* (n = 4).

Next we transplanted Kasumi-1 cells transduced with lentiviral Tet-ON vector encoding KLF4 into NSG mice. After confirming the engraftment of Kasumi-1 cells in the peripheral blood by flow cytometry, we divided engrafted mice into four groups; control group, U0126 monotherapy group, doxycycline monotherapy group and U0126 plus doxycycline combination therapy group. Compared to the modest effect of MEK inhibition or KLF4 induction monotherapy on overall survival, combination treatment of MEK inhibition plus KLF4 induction significantly prolonged the survival (Figure 53).

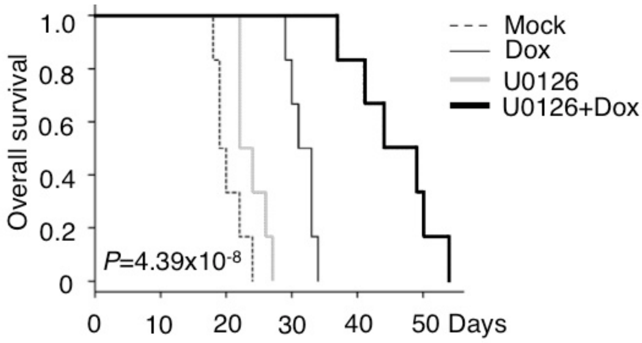


**Figure 53. MEK inhibition and KLF4 induction synergistically works against BAALC-high leukemia.**

Overall survival of NSG mice transplanted with Kasumi-1 cells transduced with Tet-ON KLF4 followed by treatment with DMSO, U0126, Dox or U0126 plus Dox (n = 6). U0126 was administered intraperitoneally at 25 μmol/kg/week and Dox was given orally (diluted in drinking water at 1 mg/mL).

These findings clearly indicate that MEK inhibition combined with KLF4 induction would be a promising therapeutic strategy against BAALC-high AML (Figure 54).

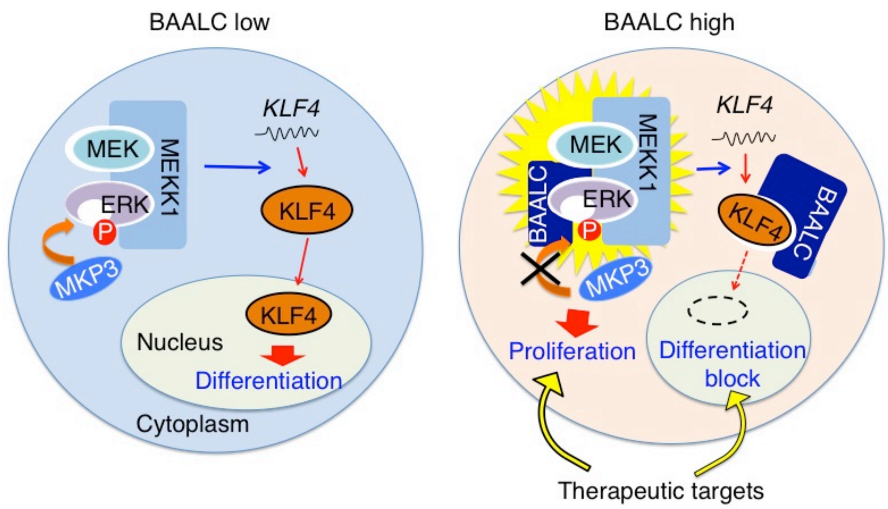

**Figure 54. Schematic summary of this study.**

BAALC interacts with MEKK1 in the cytoplasm and up-regulates ERK pathway as an adaptor protein. Constitutive activation of ERK pathway conventionally mediates monocytic differentiation via nuclear KLF4 accumulation. In contrast, in the presence of excess BAALC, KLF4 accumulation in the nucleus is blocked by cytoplasmic BAALC. Thus BAALC promotes leukemia cell proliferation by activating ERK pathway while blocking differentiation of leukemia cells by preventing ERK-pathway mediated KLF4 accumulation in the nucleus. This unique dual function of BAALC might contribute to a formation of more aggressive leukemia.

## Discussion

In this study, we showed that BAALC promotes proliferation and drug resistance of AML cells by sustained activation of ERK pathway through the interaction with MEKK1 and that BAALC inhibits monocytic differentiation induced by ERK through nucleo-cytoplasmic translocation of KLF4. We also demonstrated that inhibition of ERK pathway, especially combined with KLF4 induction, is highly effective against BAALC-high leukemia cells both in vitro and in vivo.

Our detailed experiments revealed that BAALC interacts with MEKK1, inhibits reassociation of ERK and MKP3, and consequently maintains ERK activity, which is one of the pivotal transmitters of growth-factor signaling. Sustained activation of ERK pathway promotes proliferation through cell cycle progression in AML cells. In addition, ERK-dependent up-regulation of chemoresistance-associated transporters in response to cytotoxic agents were enhanced by BAALC overexpression, indicating that BAALC mediates a variety of functions on AML cells by modulating ERK activity. Since aberrant expressions of ABC transporters are well-known markers for poor prognosis in AML patients [53, 54], molecules targeting them have been extensively searched, but yet to be discovered [55, 56]. Considering the association of higher BAALC expression among AML patients with primary refractory disease and paucity of promising drugs in clinical use targeting these chemoresistance-associated transporters, the rationality of treating BAALC-high AML with MEK inhibitors to overcome ERK-mediated drug resistance should be emphasized.

Although aberrant activation of ERK pathway is implicated in the biology of AML[15], chronic activation of ERK induced by constitutive active form of MEK1 leads AML cells to monocytic differentiation[57], suggesting an unidentified mechanism that blocks ERK-mediated differentiation of AML cells. Several genes have been implicated in the differentiation of myeloid cells such as *RUNX1*, *C/EBPα*, *PU.1* and *KLF4*[27, 58-60], but none have been identified as a key player in ERK-mediated differentiation of myeloid leukemia cells. In this report, we demonstrated that constitutively active MEK1-induced monocytic differentiation of AML cells depends on KLF4 induction, which is the other interacting partner of BAALC. In addition, we showed a unique spatiotemporal distribution of KLF4 in the presence of BAALC. BAALC inhibits the nuclear localization of KLF4 by interacting with KLF4 in the cytoplasm and hindering its nuclear translocation by immunofluorescence study. It is of note that mRNA expression levels of *BAALC* in AML cell lines with higher expression of BAALC protein utilized in our immunofluorescence study was similar to those in primary bone marrow cells from AML patients with high BAALC expression. Physiological sequestration of specific tumor suppressor proteins in the cytoplasm has been documented in several cases[61-63] and drugs targeting this subcellular protein-protein interactions do exist [64, 65]. To our knowledge, this is the first report that shows the cytoplasmic sequestration of KLF4 confers oncogenic potential. Our study also suggests that targeting KLF4 would be a rational choice for overcoming treatment-resistant BAALC-high AML.

Furthermore, our data indicated that MEK inhibition could effectively treat BAALC-high AML. Although several MEK inhibitors are already utilized in a clinical settings[66], the efficacy of MEK inhibitor monotherapy is limited so far, firstly because of the high probability of side effects due to its narrow therapeutic concentration range, and secondly because of emergence of resistance mainly due to the complex signaling networks inducing up-regulation of bypass pathways and MAPK reactivation through positive and negative feedback-loops[66]. Thus, proper and multimodal therapy is needed in most cases of malignancies treated by MEK inhibitors[67-69]. In our experiments using AML cell lines and primary human samples, AML cells with higher expression of BAALC possessed higher sensitivity to MEK inhibitor U0126. In addition, U0126 decreased the proliferation rate of leukemia cells with high BAALC expression at significantly lower concentration compared to that of BAALC-low cells. These results suggested that AML patients with higher expression of BAALC might be effectively treated by MEK inhibitor at relatively low doses, which can reduce the toxicity. Moreover, MEK inhibitor can reverse the drug resistance conferred by BAALC, which might be involved in unfavorable prognosis of BAALC-high AML patients, and can potentiate the therapeutic efficacy of other antileukemic agents. Given that U0126 cannot reverse differentiation block caused by direct interaction of BAALC with KLF4 independently from ERK, KLF4 induction therapy both in vitro and in vivo was combined with MEK inhibition in this study. Our results clearly showed that concurrent MEK inhibition and KLF4 induction are highly effective for BAALC-high AML. Several drugs which can induce KLF4 have been evaluated in clinical and preclinical settings, making our approach feasible and highly promising[29].

To date, there have been few reports that provide a perspective on the leukemogenic property of BAALC itself[70-73]. This is the first report underscoring the uniqueness of BAALC to be an unprecedented dual-acting protein which functions as an adaptor protein in MAPK cascade and as a molecular trap against KLF4 in the cytoplasm, although a physiological role of BAALC as well as KLF4 is yet to be clarified. Considering that MEK inhibition is effective for inhibiting the proliferation and drug resistance of BAALC-high leukemia cells even at lower doses and concurrent KLF4 induction further enhances therapeutic efficacy, our results strongly indicate that combination therapy targeting this novel BAALC-ERK-KLF4 axis would become a promising strategy for refractory AML with high BAALC expression.

**Acknowledgements**

I express my hearty thanks to Professor Mineo Kurokawa (Department of Hematology & Oncology, Graduate School of Medicine, the University of Tokyo, Tokyo, Japan) for the leadership and advices. I also extend my gratitude to Dr. Y Masamoso, Dr. K Kataoka, Dr. J Koya, Dr. Y Kagoya, Dr. T Sato (Department of Hematology & Oncology, Graduate School of Medicine, the University of Tokyo, Tokyo, Japan), Dr. H Yashiroda and Dr. S Murata (Laboratory of Protein Metabolism, Graduate School of Pharmaceutical Sciences, the University of Tokyo, Tokyo, Japan) for meaningful advices. I thank Dr. T. Kitamura (The Institute of Medical Sciences, The University of Tokyo, Tokyo, Japan) for platinum-A (Plat-A) packaging cells, and lentivirus vectors of CSII-EF-MCS-IRES2-Venus, CSII-EF-MCS-IRES2-hKO1, pENTR4-H1tetOx1, CSIV-TRE-RfA-EF-KT, psPAX2 and pMD2.G for Dr. H. Miyoshi (RIKEN BioResource Center, Ibaragi, Japan). I also thank Dr. E. Takekawa (The Institute of Medical Sciences, The University of Tokyo, Tokyo, Japan) for cDNA construct of CA-MEK1, MEKK1, Dr. T. Furukawa (Tokyo Women's Medical University, Tokyo, Japan) for MKP3, Dr. S. Yamanaka (The Center for iPS Cell Research and Application

(CiRA), Kyoto, Japan) for KLF4, and Dr. A. de la Chapelle (The Ohio State University, Ohio, USA) for BAALC respectively.

**References**

1. Rowe, J.M. & Tallman, M.S. How I treat acute myeloid leukemia. *Blood* **116**, 3147-3156 (2010).

2. Ferrara, F. & Schiffer, C.A. Acute myeloid leukaemia in adults. *Lancet* **381**, 484-495 (2013).

3. Abdel-Wahab, O. *et al.* ASXL1 mutations promote myeloid transformation through loss of PRC2-mediated gene repression. *Cancer Cell* **22**, 180-193 (2012).

4. Ko, M. *et al.* Impaired hydroxylation of 5-methylcytosine in myeloid cancers with mutant TET2. *Nature* **468**, 839-843 (2010).

5. Ley, T.J. *et al.* DNMT3A mutations in acute myeloid leukemia. *N Engl J Med* **363**, 2424-2433 (2010).

6. Marcucci, G. *et al.* High expression levels of the ETS-related gene, ERG, predict adverse outcome and improve molecular risk-based classification of cytogenetically normal acute myeloid leukemia: a Cancer and Leukemia Group

B Study. *J Clin Oncol* **25**, 3337-3343 (2007).

7. Gröschel, S. *et al.* High EVI1 expression predicts outcome in younger adult patients with acute myeloid leukemia and is associated with distinct cytogenetic abnormalities. *J Clin Oncol* **28**, 2101-2107 (2010).

8. Heuser, M. *et al.* High meningioma 1 (MN1) expression as a predictor for poor outcome in acute myeloid leukemia with normal cytogenetics. *Blood* **108**, 3898-3905 (2006).

9. Baldus, C.D. *et al.* BAALC expression predicts clinical outcome of de novo acute myeloid leukemia patients with normal cytogenetics: a Cancer and Leukemia Group B Study. *Blood* **102**, 1613-1618 (2003).

10. Tanner, S.M. *et al.* BAALC, the human member of a novel mammalian neuroectoderm gene lineage, is implicated in hematopoiesis and acute leukemia. *Proc Natl Acad Sci U S A* **98**, 13901-13906 (2001).

11. Langer, C. *et al.* High BAALC expression associates with other molecular prognostic markers, poor outcome, and a distinct gene-expression signature in cytogenetically normal patients younger than 60 years with acute myeloid

leukemia: a Cancer and Leukemia Group B (CALGB) study. *Blood* **111**, 5371-5379 (2008).

12. Baldus, C.D. *et al.* BAALC expression and FLT3 internal tandem duplication mutations in acute myeloid leukemia patients with normal cytogenetics: prognostic implications. *J Clin Oncol* **24**, 790-797 (2006).

13. Damiani, D. *et al.* BAALC overexpression retains its negative prognostic role across all cytogenetic risk groups in acute myeloid leukemia patients. *Am J Hematol* **88**, 848-852 (2013).

14. Baldus, C.D. *et al.* BAALC, a novel marker of human hematopoietic progenitor cells. *Exp Hematol* **31**, 1051-1056 (2003).

15. Blume-Jensen, P. & Hunter, T. Oncogenic kinase signalling. *Nature* **411**, 355-365 (2001).

16. Towatari, M. *et al.* Constitutive activation of mitogen-activated protein kinase pathway in acute leukemia cells. *Leukemia* **11**, 479-484 (1997).

17. Lunghi, P. *et al.* Downmodulation of ERK activity inhibits the proliferation and induces the apoptosis of primary acute myelogenous leukemia blasts. *Leukemia*

**17**, 1783-1793 (2003).

18. Jain, N. *et al.* Phase II study of the oral MEK inhibitor selumetinib in advanced acute myelogenous leukemia: a University of Chicago phase II consortium trial. *Clin Cancer Res* **20**, 490-498 (2014).

19. Karandikar, M., Xu, S. & Cobb, M.H. MEKK1 binds raf-1 and the ERK2 cascade components. *J Biol Chem* **275**, 40120-40127 (2000).

20. Jin, J.O., Song, M.G., Kim, Y.N., Park, J.I. & Kwak, J.Y. The mechanism of fucoidan-induced apoptosis in leukemic cells: involvement of ERK1/2, JNK, glutathione, and nitric oxide. *Mol Carcinog* **49**, 771-782 (2010).

21. Nakamura, Y., Yujiri, T., Nawata, R., Tagami, K. & Tanizawa, Y. MEK kinase 1 is essential for Bcr-Abl-induced STAT3 and self-renewal activity in embryonic stem cells. *Oncogene* **24**, 7592-7598 (2005).

22. Santos, S.D., Verveer, P.J. & Bastiaens, P.I. Growth factor-induced MAPK network topology shapes Erk response determining PC-12 cell fate. *Nat Cell Biol* **9**, 324-330 (2007).

23. Deschênes-Simard, X. *et al.* Tumor suppressor activity of the ERK/MAPK

pathway by promoting selective protein degradation. *Genes Dev* **27**, 900-915 (2013).

24. Bric, A. *et al.* Functional identification of tumor-suppressor genes through an in vivo RNA interference screen in a mouse lymphoma model. *Cancer Cell* **16**, 324-335 (2009).

25. Chen, Z.Y. & Tseng, C.C. 15-deoxy-Delta12,14 prostaglandin J2 up-regulates Kruppel-like factor 4 expression independently of peroxisome proliferator-activated receptor gamma by activating the mitogen-activated protein kinase kinase/extracellular signal-regulated kinase signal transduction pathway in HT-29 colon cancer cells. *Mol Pharmacol* **68**, 1203-1213 (2005).

26. Okita, K., Ichisaka, T. & Yamanaka, S. Generation of germline-competent induced pluripotent stem cells. *Nature* **448**, 313-317 (2007).

27. Feinberg, M.W. *et al.* The Kruppel-like factor KLF4 is a critical regulator of monocyte differentiation. *EMBO J* **26**, 4138-4148 (2007).

28. Faber, K. *et al.* CDX2-driven leukemogenesis involves KLF4 repression and deregulated PPARγ signaling. *J Clin Invest* **123**, 299-314 (2013).

29. Cho, S.D. *et al.* 5,5'-Dibromo-bis(3'-indolyl)methane induces Kruppel-like factor 4 and p21 in colon cancer cells. *Mol Cancer Ther* **7**, 2109-2120 (2008).

30. Chintharlapalli, S. *et al.* 2-cyano-lup-1-en-3-oxo-20-oic acid, a cyano derivative of betulinic acid, activates peroxisome proliferator-activated receptor gamma in colon and pancreatic cancer cells. *Carcinogenesis* **28**, 2337-2346 (2007).

31. Lyssiotis, C.A. *et al.* Reprogramming of murine fibroblasts to induced pluripotent stem cells with chemical complementation of Klf4. *Proc Natl Acad Sci U S A* **106**, 8912-8917 (2009).

32. Ghosh, A. & Pahan, K. Gemfibrozil, a lipid-lowering drug, induces suppressor of cytokine signaling 3 in glial cells: implications for neurodegenerative disorders. *J Biol Chem* **287**, 27189-27203 (2012).

33. Rowland, B.D., Bernards, R. & Peeper, D.S. The KLF4 tumour suppressor is a transcriptional repressor of p53 that acts as a context-dependent oncogene. *Nat Cell Biol* **7**, 1074-1082 (2005).

34. Chou, T.C. & Talalay, P. Quantitative analysis of dose-effect relationships: the

combined effects of multiple drugs or enzyme inhibitors. *Adv Enzyme Regul* **22**, 27-55 (1984).

35. Kim, M.O. *et al.* ERK1 and ERK2 regulate embryonic stem cell self-renewal through phosphorylation of Klf4. *Nat Struct Mol Biol* **19**, 283-290 (2012).

36. Wang, X. *et al.* BAALC 1-6-8 protein is targeted to postsynaptic lipid rafts by its N-terminal myristoylation and palmitoylation, and interacts with alpha, but not beta, subunit of Ca/calmodulin-dependent protein kinase II. *J Neurochem* **92**, 647-659 (2005).

37. Russell, M., Lange-Carter, C.A. & Johnson, G.L. Direct interaction between Ras and the kinase domain of mitogen-activated protein kinase kinase kinase (MEKK1). *J Biol Chem* **270**, 11757-11760 (1995).

38. Shields, J.M. & Yang, V.W. Two potent nuclear localization signals in the gut-enriched Krüppel-like factor define a subfamily of closely related Krüppel proteins. *J Biol Chem* **272**, 18504-18507 (1997).

39. Alcorta, D.A. *et al.* Sequence and expression of chicken and mouse rsk: homologs of Xenopus laevis ribosomal S6 kinase. *Mol Cell Biol* **9**, 3850-3859

(1989).

40. Kim, Y., Rice, A.E. & Denu, J.M. Intramolecular dephosphorylation of ERK by MKP3. *Biochemistry* **42**, 15197-15207 (2003).

41. Favata, M.F. *et al.* Identification of a novel inhibitor of mitogen-activated protein kinase kinase. *J Biol Chem* **273**, 18623-18632 (1998).

42. Santamaría, C. *et al.* BAALC is an important predictor of refractoriness to chemotherapy and poor survival in intermediate-risk acute myeloid leukemia (AML). *Ann Hematol* **89**, 453-458 (2010).

43. Abrams, S.L. *et al.* The Raf/MEK/ERK pathway can govern drug resistance, apoptosis and sensitivity to targeted therapy. *Cell Cycle* **9**, 1781-1791 (2010).

44. McCubrey, J.A. *et al.* Involvement of p53 and Raf/MEK/ERK pathways in hematopoietic drug resistance. *Leukemia* **22**, 2080-2090 (2008).

45. Chang, G. Multidrug resistance ABC transporters. *FEBS Lett* **555**, 102-105 (2003).

46. Shen, H. *et al.* Upregulation of mdr1 gene is related to activation of the MAPK/ERK signal transduction pathway and YB-1 nuclear translocation in

B-cell lymphoma. *Exp Hematol* **39**, 558-569 (2011).

47. El Azreq, M.A., Naci, D. & Aoudjit, F. Collagen/β1 integrin signaling up-regulates the ABCC1/MRP-1 transporter in an ERK/MAPK-dependent manner. *Mol Biol Cell* **23**, 3473-3484 (2012).

48. Imai, Y. *et al.* Breast cancer resistance protein/ABCG2 is differentially regulated downstream of extracellular signal-regulated kinase. *Cancer Sci* **100**, 1118-1127 (2009).

49. Lai, J.K. *et al.* Krüppel-like factor 4 is involved in cell scattering induced by hepatocyte growth factor. *J Cell Sci* **125**, 4853-4864 (2012).

50. Alder, J.K. *et al.* Kruppel-like factor 4 is essential for inflammatory monocyte differentiation in vivo. *J Immunol* **180**, 5645-5652 (2008).

51. Musgrove, E.A., Caldon, C.E., Barraclough, J., Stone, A. & Sutherland, R.L. Cyclin D as a therapeutic target in cancer. *Nat Rev Cancer* **11**, 558-572 (2011).

52. Rowland, B.D. & Peeper, D.S. KLF4, p21 and context-dependent opposing forces in cancer. *Nat Rev Cancer* **6**, 11-23 (2006).

53. van den Heuvel-Eibrink, M.M. *et al.* CD34-related coexpression of MDR1 and

BCRP indicates a clinically resistant phenotype in patients with acute myeloid leukemia (AML) of older age. *Ann Hematol* **86**, 329-337 (2007).

54. Schaich, M. *et al.* MDR1 and MRP1 gene expression are independent predictors for treatment outcome in adult acute myeloid leukaemia. *Br J Haematol* **128**, 324-332 (2005).

55. Mahadevan, D. & List, A.F. Targeting the multidrug resistance-1 transporter in AML: molecular regulation and therapeutic strategies. *Blood* **104**, 1940-1951 (2004).

56. van der Holt, B. *et al.* The value of the MDR1 reversal agent PSC-833 in addition to daunorubicin and cytarabine in the treatment of elderly patients with previously untreated acute myeloid leukemia (AML), in relation to MDR1 status at diagnosis. *Blood* **106**, 2646-2654 (2005).

57. Miranda, M.B., McGuire, T.F. & Johnson, D.E. Importance of MEK-1/-2 signaling in monocytic and granulocytic differentiation of myeloid cell lines. *Leukemia* **16**, 683-692 (2002).

58. Goyama, S. *et al.* Transcription factor RUNX1 promotes survival of acute

myeloid leukemia cells. *J Clin Invest* **123**, 3876-3888 (2013).

59. Koleva, R.I. *et al.* C/EBPα and DEK coordinately regulate myeloid differentiation. *Blood* **119**, 4878-4888 (2012).

60. Nerlov, C. & Graf, T. PU.1 induces myeloid lineage commitment in multipotent hematopoietic progenitors. *Genes Dev* **12**, 2403-2412 (1998).

61. Vallentin, A., Prévostel, C., Fauquier, T., Bonnefont, X. & Joubert, D. Membrane targeting and cytoplasmic sequestration in the spatiotemporal localization of human protein kinase C alpha. *J Biol Chem* **275**, 6014-6021 (2000).

62. Becker, K., Marchenko, N.D., Maurice, M. & Moll, U.M. Hyperubiquitylation of wild-type p53 contributes to cytoplasmic sequestration in neuroblastoma. *Cell Death Differ* **14**, 1350-1360 (2007).

63. Kim, J. *et al.* Cytoplasmic sequestration of p27 via AKT phosphorylation in renal cell carcinoma. *Clin Cancer Res* **15**, 81-90 (2009).

64. Lång, E. *et al.* The arsenic-based cure of acute promyelocytic leukemia promotes cytoplasmic sequestration of PML and PML/RARA through

inhibition of PML body recycling. *Blood* **120**, 847-857 (2012).

65. Walker, C., Böttger, S. & Low, B. Mortalin-based cytoplasmic sequestration of p53 in a nonmammalian cancer model. *Am J Pathol* **168**, 1526-1530 (2006).

66. Akinleye, A., Furqan, M., Mukhi, N., Ravella, P. & Liu, D. MEK and the inhibitors: from bench to bedside. *J Hematol Oncol* **6**, 27 (2013).

67. Zhao, Y. & Adjei, A.A. The clinical development of MEK inhibitors. *Nat Rev Clin Oncol* **11**, 385-400 (2014).

68. Neuzillet, C. *et al.* MEK in cancer and cancer therapy. *Pharmacol Ther* **141**, 160-171 (2014).

69. Gysin, S., Salt, M., Young, A. & McCormick, F. Therapeutic strategies for targeting ras proteins. *Genes Cancer* **2**, 359-372 (2011).

70. Eisfeld, A.K. *et al.* miR-3151 interplays with its host gene BAALC and independently affects outcome of patients with cytogenetically normal acute myeloid leukemia. *Blood* **120**, 249-258 (2012).

71. Eisfeld, A.K. *et al.* Intronic miR-3151 within BAALC drives leukemogenesis by deregulating the TP53 pathway. *Sci Signal* **7**, ra36 (2014).

72. Eisfeld, A.K. *et al.* Heritable polymorphism predisposes to high BAALC expression in acute myeloid leukemia. *Proc Natl Acad Sci U S A* **109**, 6668-6673 (2012).

73. Heuser, M. *et al.* Functional role of BAALC in leukemogenesis. *Leukemia* **26**, 532-536 (2012).

**Table 1**

**PCR primers used for RT-PCR.**

| | Forward (5' → 3') | Reverse (5' → 3') |
|---|---|---|
| BAALC | AAGGCACCAACAGATTCA | AAGGCCATTCTGTTTCTG |
| CES1 | GAACCACAGAGATGCTGGAGC | TCCCCGTGGTCTCCTATCAC |
| CSF1R | GAGCGACGTCTGGTCCTATG | AGGATGCCAGGGTAGGGATT |
| MAFB | CTCAGCACTCCGTGTAGCTC | GTAGTTGCTCGCCATCCAGT |
| GAPDH | CATGTTCGTCATGGGGTGAACCA | AGTGATGGCATGGACTGTGGTCAT |
| ABCB1 | CAGGAACCTGTATTGTTTGCCACCAC | TGCTTCTGCCCACCACTCAACTG |
| ABCC1 | ACCCTAATCCCTGCCCAGAG | CGCATTCCTTCTTCCAGTTC |
| ABCC2 | ACGGGCACATCACCATCAAG | CTCCAGGCAGCATTTCCAAG |
| ABCC3 | CGCCTGTTTTTCTGGTGGTT | TTGTGTCGTGCCGTCTGCTT |
| ABCC4 | GCGGCTGACGGTTACCCTCTT | TCTGATGCCTTATCCCAAAAAGCAGT |
| ABCC5 | CCAAGCTGACCCCCAAAATGAAAAA | TGGATGTGCTTGCCTTCTTCCTCTTC |
| ABCG2 | GGTGGAGGCAAATCTTCGTTATTAGA | GAGTGCCCATCACAACATCATCTT |
| CDK2 | GCCAGAAACAAGTTGACGGGAGA | TGGGTGTAAGTACGAACAGGGAC |
| CDK4 | CTGTGGACATGTGGAGTGTTG | GGCAGAGATTCGCTTGTGTG |
| CDK6 | TGCACAGTGTCACGAACAGA | ACCTCGGAGAAGCTGAAACA |
| CCND1 | CTTCCTCTCCAAAATGCCAG | AGAGATGGAAGGGGGAAAGA |
| CDKN1A | GAGGCCGGGATGAGTTGGGAGGAG | CAGCCGGCGTTTGGAGTGGTAGAA |
| CDKN1B | AGACGGGGTTAGCGGAGCAA | TCTTGGGCGTCTGCTCCACA |

**Table 2**

**Target sequences used for shRNA knockdown experiments.**

| | 5’ → 3’ |
|---|---|
| sh_*BAALC*#1 | GAGACTGAATTAGACCCT |
| sh_*BAALC*#2 | TCACAAAGAACTGTGTCAA |
| sh_*KLF4* | GCTCCATTACCAAGAGCTCAT |
| sh_*Luc.* | CGTACGCGGAATACTTCGA |